

1 **Intelligent Traffic Organization for Sea Ports: Fusing Multi-Source**

2 **Data for Resource Allocation and Scheduling**

3 Yang Liu ^{a, b}, Jingxian Liu ^{a, c}, Qian Zhang ^{d, *}, Yi Liu ^{a, c*}, Yukuan Wang ^{a, c}, Lichao Yang ^{a, c}

4 *a (State Key Laboratory of Maritime Technology and Safety, Wuhan University of Technology,*
5 *Wuhan, 430063, China)*

6 *b (Intelligent Transportation Systems Research Center, Wuhan University of Technology, 1040*
7 *Heping Avenue, Wuhan, Hubei 430063, China)*

8 *c (School of Navigation, Wuhan University of Technology, 430063, China)*

9 *d (School of Engineering, Liverpool John Moores University, Liverpool, L3 3AF, UK)*

10 **Abstract:** Reliable autonomous traffic organization is critical for smart ports operating under
11 dynamic ocean conditions. This study proposes a comprehensive framework for sea port
12 scheduling based on Multi-Source Information Fusion (MSIF). To address the challenge of fusing
13 heterogeneous data streams-including vessel trajectories, resource availability, and environmental
14 constraints-a Mixed-Integer Programming (MIP) formulation is first established. Subsequently, a
15 high-fidelity digital twin integrating Cellular Automata (CA) and Multi-Agent Systems (MAS) is
16 developed to simulate heterogeneous cooperative behaviours and stochastic uncertainties.
17 Crucially, a novel Simulation-based Multi-Objective Genetic Algorithm (SMOGA) serves as the
18 autonomous decision-making engine, fusing simulation feedback with evolutionary search to
19 optimize vessel sequencing and resource allocation dynamically. Validated with real-world data
20 from Tianjin Port, the framework outperforms both traditional rules and modern swarm
21 intelligence algorithms, increasing throughput by 16.5% and reducing turnaround time by 11.7%.
22 This research demonstrates how fusing multi-scale information into an intelligent evolutionary
23 framework enables robust, autonomous decision-making in congested maritime environments.

24 **Keywords:** Autonomous Systems; Multi-Source Information Fusion; Port Traffic
25 Management; Simulation-based Multi-Objective Genetic Algorithm (SMOGA); Cooperative
26 Autonomy

27 1. Introduction

28 Maritime transportation plays a pivotal role in the global economy, accounting for over 80%
29 of the world's trade as highlighted by the United Nations Conference on Trade and Development
30 (*Towards a green and just transition*, 2023). This significant reliance on maritime transport
31 underscores the critical importance of efficient and autonomous port operations. The urgency for
32 intelligent optimization becomes particularly evident considering the substantial costs incurred by
33 vessel operators, which, as noted by Al-Dhaheri and Diabat (2017), can escalate to as much as
34 4000 USD per hour during port waiting times. These delays not only impact the profitability of
35 shipping companies but also indicate a failure in processing complex environmental data, leading
36 to congestion and inefficiencies. Additionally, the financial implications for seaport operators are
37 considerable. The cost of constructing berths and acquiring resources represents a massive capital
38 investment. Therefore, the efficient utilization of these resources through robust Multi-Source
39 Information Fusion (MSIF) is paramount to maintaining economic viability. Ineffective resource

40 allocation and traffic organisation often stem from a lack of integrated situational awareness,
41 leading to operational bottlenecks and diminishing the quality of service.

42 However, conventional optimization approaches often struggle to capture the full complexity
43 of modern seaports operating under dynamic ocean conditions. They typically focus on isolated
44 sub-problems — such as berth allocation or channel scheduling — and rely on simplified
45 mathematical models. These models frequently fail to fuse the stochastic elements inherent in
46 maritime traffic, such as unpredictable vessel arrival times, sensor data noise, and environmental
47 disruptions. Furthermore, disparate data sources regarding channel status, pilot availability, and
48 vessel dynamics are often treated independently, making it difficult to simultaneously balance
49 conflicting objectives like minimizing waiting times while ensuring safety. This disconnection
50 between simplified models and the complex, multi-source reality limits the practical applicability
51 of their solutions in autonomous systems.

52 To address these challenges, this study formulates the port traffic organization problem as a
53 comprehensive multi-objective optimization task driven by multi-source information fusion. The
54 core decision variables optimized in the proposed autonomous framework include: (1) the
55 sequence of vessel entry and exit, determining the priority of service based on fused traffic data; (2)
56 the specific arrival time at the anchorage, regulating the flow of incoming traffic; and (3) the
57 waiting duration at both anchorage and berths, which acts as a buffer against the uncertainty in
58 resource availability. By dynamically adjusting these variables, the SMOGA (Simulation-based
59 Multi-Objective Genetic Algorithm) framework aims to achieve three key objectives: maximizing
60 throughput, minimizing the peak usage of auxiliary resources, and reducing the average vessel
61 turnaround time.

62 This paper proposes a strictly validated framework to the field of maritime logistics and
63 autonomous systems by addressing the intricate challenges of traffic organisation and resource
64 allocation in busy port waters. The key contributions are as follows:

65 a. The development of a MIP model tailored for busy waterways, which comprehensively
66 fuses the constraints of various multi-source inputs within the port navigation system. This
67 includes anchorage capacities, channel rules, berth status, and dynamic auxiliary resources (pilots
68 and tugboats). The model adeptly integrates these diverse information sources, offering a holistic
69 approach to optimising traffic organisation in congested maritime environments.

70 b. The establishment of a port navigation simulation model, innovatively utilising Cellular
71 Automaton (CA) and a Multi-Agent System (MAS) approach. This model serves as a cooperative
72 autonomy framework, facilitating interactive information exchange among different resource
73 modules to manage complex constraints. Significantly, it models the uncertainty in ship waiting
74 times and dynamic conditions, thus enhancing the feasibility and practicality of the proposed
75 optimization solutions under real-world ocean environments.

76 c. The introduction of a novel solution framework that synergises Genetic Algorithms (GA)
77 with the simulation model in an iterative process. This framework seeks the optimal allocation of
78 auxiliary resources and ship autonomous scheduling under fixed capacities of anchorage, channels,
79 and berths. It achieves multi-objective optimization of resources and autonomous scheduling in
80 port traffic organisation, thereby presenting new perspectives and methodologies for intelligent
81 port management.

82 The research methodology employed in this study is depicted in Fig. 1. The subsequent
83 sections are organized as follows: Section 2 highlights the most recent research gaps in related
84 fields, Section 3 describes the optimization problem associated with seaport organisation, Section
85 4 presents a solution approach based on simulation modelling and Genetic Algorithms (GA),
86 Section 5 applies the model to Tianjin Port for empirical validation, and Section 6 discusses the
87 model and proposes directions for future research.

Simulation-based Multi-Objective Genetic Algorithm (SMOGA)

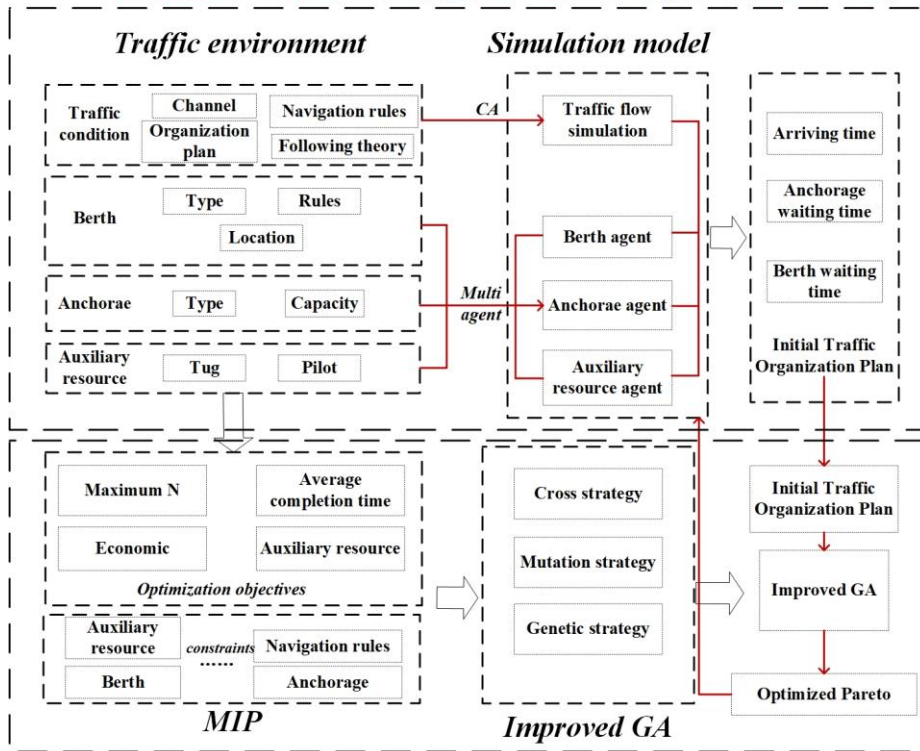


Fig. 1. Logical structure of the study

88

89

90 2. Literature Review

91 The present paper integrates heuristic optimization algorithms with traffic simulation models
 92 to address the multi-objective optimization problem of auxiliary resource allocation and ship
 93 scheduling in port traffic systems. The review section is organized into three parts: traffic
 94 organisation optimization, traffic simulation models regarding heterogeneous flows, and
 95 multi-source information fusion in the context of maritime IoT.

96 2.1 Traffic organisation optimization problem of port navigation system

97 Current studies on ship traffic organisation in ports extend beyond basic operations to
 98 specific domains such as ship route optimization (W. Chen et al., 2023; Karimi et al., 2025; M. Li
 99 et al., 2022; Norstad et al., 2011; Zhen et al., 2020), Ship speed optimization (Luo et al., 2024;
 100 Psaraftis and Kontovas, 2014; Wang et al., 2018), sea-rail intermodal transportation (Fan et al.,
 101 2019), berth allocation problem (Hsu, 2016), and Port State Control (PSC) inspection optimization
 102 (Yan et al., 2024; Yang et al., 2024), current studies on ship traffic organisation in ports mainly
 103 concentrate on tugboat resources, pilot resources, ship collision avoidance and ship scheduling
 104 arrangements (Ma et al., 2024; Sun et al., 2025; Wang et al., 2024).

105 Initially, scholars explored various methodological approaches. Fagerholt (2001) addressed
 106 ship scheduling as a multiple ship pickup and delivery problem with soft time windows
 107 (m-PDPSTW). Aydogdu (2012) proposed a management-oriented solution for the Istanbul Strait
 108 considering spatial-temporal distribution. Smierzchalski (2000) focused on autonomous route
 109 selection using evolutionary algorithms, while Kawaguchi et al. (2009) introduced a ship cluster
 110 behaviour model to maximize waterway resource utilization.

111 Subsequently, the focus shifted towards Mixed-Integer Programming (MIP) models. Corry et
 112 al. (2019) integrated channel movement scheduling with berth allocation. Jia et al. (2022, 2020,
 113 2019) provided MIP formulations to optimize pilot and ship costs, balancing efficiency and
 114 fairness. Kang et al. (2020) attempted to optimize container ship schedules using simulation

115 methods. Other significant contributions include Li et al. (2019) on minimizing berthing delays,
116 Wei et al. (2020) on tugboat scheduling, and Wu et al. (2020) on pilotage planning, demonstrating
117 the NP-hard nature of these problems. Further advancements by Abou et al. (2021) and Liu et al.
118 (2021b, 2021a) incorporated complex constraints like channel restrictions and one-way navigation.
119 Recent studies have also addressed emissions via speed reduction (Xiao et al., 2021), uncertainty
120 analysis (Ksciuka et al., 2023) and optimal control for path planning (Shu et al., 2024). With the
121 rapid development of the electric vehicle industry, the traffic organization of roll-on/roll-off
122 (Ro-Ro) ship liner routes carrying both electric and gasoline vehicles has also begun to attract
123 attention (Wang et al., 2026). Despite this extensive body of work, there remains a noticeable
124 scarcity of research specifically targeting autonomous vessel traffic organization, particularly
125 frameworks that can dynamically adapt to the stochastic nature of future smart ports.

126 **2.2 Port navigation system traffic simulation model**

127 Currently, in the domain of waterway traffic, a predominant number of scholars have
128 embarked on developing simulation models based on CA. Liu et al. (2010), utilizing diverse ship
129 categories, safety distances, ship arrival patterns, and berth service levels, developed a CA model
130 to simulate port waterway traffic flows. This model adeptly navigated the complexities and
131 non-linear challenges associated with simulation. Following this, various researchers have
132 incorporated random variables into the CA framework to simulate ship traffic flows. This
133 integration aims to capture the impact of environmental factors on maritime movements, as
134 outlined in studies by Qi et al. (2017; Zhen et al., 2017) and Qu et al. (2012). With increased
135 activity in the approach channels, investigations into the effects of lane switching on traffic
136 efficiency have been undertaken, as demonstrated in research by Sun et al. (2015), Hu et al. (2017),
137 and Qi et al. (2021), Chen et al. (2023) and others established a ship traffic flow simulation model
138 for narrow channels under the premise of considering navigation rules.

139 Concurrently, the application of multi-agent simulation technology (Zhang et al., 2005) in the
140 field of transportation has been rapidly evolving. With the demand for higher precision,
141 Multi-Agent Systems (MAS) have been integrated with CA. Jiang et al. (2019) combined CA with
142 MAS to explore ship behaviour impacts on port operations, and Liu et al. (2021) applied this
143 paradigm to LNG carrier movements.

144 Regarding heterogeneous traffic flow, extensive research exists in road transportation (Fan et
145 al., 2025; Jin et al., 2025; L. Li et al., 2022; Yao et al., 2023). However, in the maritime domain,
146 research on the coexistence of autonomous and manned vessels is emerging. Notably, Liu et al.
147 (2024a, 2024b) developed a heterogeneous traffic flow simulation model based on CA, providing
148 a foundation for analysing the interaction between autonomous and conventional ships in port
149 waters.

150 **2.3 Multi-Source Information Fusion (MSIF) and Maritime IoT**

151 As port management evolves towards intelligence, the integration of the Internet of
152 Things (IoT) and Multi-Source Information Fusion (MSIF) has become critical for top-level
153 smart port design. Recent literature highlights how fusing diverse data streams enhances
154 situational awareness and decision-making.

155 Liu et al. (2022a) proposed an edge computing method based on multi-source
156 information fusion to serve autonomous vessels within the Maritime IoT (MIoT) framework.
157 Similarly, Xiao et al. (2023) developed a trajectory prediction neural network driven by
158 multi-source data fusion for intelligent traffic systems. Specific applications of deep learning
159 in this context include ship trajectory prediction for port management (Liu et al., 2022b), and
160 ship speed interval prediction under MIoT (Liu et al., 2025). Furthermore, to enhance visual

161 perception in smart ports, Lu et al. (2023; 2024; 2022) proposed a series of deep
162 learning-based image enhancement methods. Complementing these analytical tools, Liang et
163 al. (2025) introduced a rapid visualization method for massive data in MIoT. These studies
164 collectively demonstrate the growing importance of fusing AIS data, visual data, and sensor
165 inputs; however, the application of MSIF specifically for optimizing traffic scheduling logic
166 remains underexplored.

167 **2.3 Research gap**

168 An analysis of existing research reveals three primary areas necessitating refinement: a.
169 Integration of MSIF in Scheduling: While MSIF is widely used for prediction and perception (as
170 discussed in Section 2.3), it is rarely directly integrated into the optimization loop of traffic
171 organization algorithms. b. Autonomous Organization: Existing MIP models (Section 2.1)
172 typically rely on centralized, static planning and lack the adaptive mechanisms required for
173 autonomous vessel traffic organization. c. Simulation as an Optimizer: While simulation models
174 (Section 2.2) effectively mimic heterogeneous flows, they are often used for evaluation rather than
175 as an active component of the optimization process.

176 **3. Problem description**

177 The optimization problem of traffic organisation within port navigation systems may be
178 characterised as a quintessential multi-objective, MIP problem. This section introduces,
179 respectively, the process of traffic organisation and the optimization challenges inherent in port
180 navigation systems, culminating in a multi-objective, mixed-integer programming model.

181 **3.1 Traffic organisation**

182 In this study, we meticulously examine the complete process of ship entry and departure from
183 ports, focusing primarily on nautical aspects. The port resources involved in this process
184 encompass anchorages, inbound and outbound channels, and berths, supplemented by auxiliary
185 resources such as pilots and tugboats, in addition to shore-based support personnel. The detailed
186 process for ship port entry and departure is as follows:

187 a. Ships first arrive at the anchorage, awaiting the availability of free berths as well as pilot
188 and tugboat resources. The resource occupancy is contingent on the ship type, and upon
189 satisfaction of these resource requirements, ships proceed to the inbound channel.

190 b. During the navigation phase within the inbound channel, ship speed is dependent on the
191 type of ship and must also account for interactions with preceding and following ships.

192 c. Upon reaching the berth, cargo loading and unloading operations commence, the duration
193 of which varies with the ship type. Similarly, for departure, the availability of sufficient free
194 auxiliary resources is considered before ships embark on the outbound channel.

195 d. The outbound navigation process mirrors that of the inbound phase.

196 f. The waiting time of ships is affected by random factors: the availability of pilot/tug
197 resources follows an exponential distribution, and the passage time of the channel is affected by
198 the interaction of ships.

199 To clarify the terminology used throughout this framework, we define the hierarchical
200 relationship as follows: “Traffic Organization” refers to the holistic management strategy for the
201 entire port ecosystem, including rule formulation and resource coordination. “Scheduling” denotes
202 the specific, tactical execution of this strategy, manifesting as the precise temporal assignment of
203 vessels to channels, anchorages, and berths. The proposed framework utilizes autonomous
204 scheduling to achieve efficient traffic organization. To formulate the intelligent traffic organization
205 problem, this study operates under the hypothetical premise of a Level 4 Autonomous Port

206 environment. Specifically, we assume:

207 1. Full Connectivity: All vessels and port infrastructure are equipped with V2X
 208 (Vehicle-to-Everything) communication capabilities, enabling real-time data exchange
 209 regarding position, speed, and intent.

210 2. Digital Transparency: The status of auxiliary resources (pilots/tugs) and anchorages is
 211 digitized and broadcasted in real-time. These premises allow the proposed system to
 212 transition from traditional voice-based dispatching to data-driven digital scheduling.

213 Throughout the entire port entry and departure process, numerous uncertainties exist, with the
 214 most prominent being: the indeterminacy of ship waiting times at anchorages and berths due to
 215 resource constraints, and the uncertainty in navigation time within channels owing to ship speed
 216 and interactions. These elements of uncertainty significantly compound the complexity of
 217 optimising traffic organisation in port navigation systems.

218 3.2. Mixed-integer programming problem

219 To address the issue of traffic organisation optimization in port navigation systems, we have
 220 established a MIP model. This model is meticulously structured, with clearly defined parameters
 221 tailored to encapsulate the multifaceted aspects of port traffic dynamics. The formulation of the
 222 model is as follows:

223 Firstly, the model incorporates a comprehensive set of parameters that represent the critical
 224 elements of port traffic (**Table 1**), such as the number and types of ships, berth allocation, arrival
 225 and departure times, and resource availability (including tugs and pilots).

226 The essence of Multi-Source Information Fusion lies in the dynamic mapping of
 227 heterogeneous data streams into the MIP model parameters. Specifically, real-time AIS data
 228 determines the set of ships I and their initial states (Arrival Time); the dynamic status updates of
 229 pilots and tugs directly quantify the resource capacity bounds P and G (Eq. 4-5); and
 230 environmental sensor data updates the channel capacity constraints (C_{in}, C_{out}). This fusion ensures
 231 that the mathematical constraints strictly reflect the physical reality of the port.

232 **Table1**

233 Parameters and Decision Variables

Category	Symbol	Description
Sets:	I	The set of all ships, indexed by $i \in I$.
	T	The set of time steps over the planning horizon, indexed by $t \in T$.
	P	The set of all pilots, indexed by $p \in P$.
	G	The set of all tugboats, indexed by $g \in G$.
Parameters:		
	n	Total number of ships.
	$\ P\ $	Total number of available pilots.
	$\ G\ $	Total number of available tugboats.
	A_{cap}	Maximum capacity of the anchorage (number of ships).
	B_{cap}	Maximum capacity of the berths (number of ships).
	C_{in}	Maximum capacity of the inbound channel (number of ships at the same time).
	C_{out}	Maximum capacity of the outbound channel (number of ships at the same time).
	t_c	The time required for a ship to continuously navigate the channel.

P_i^{req}	Number of pilots required by ship i
G_i^{req}	Number of tugboats required by ship i
E	Economic indicators

Decision
variables:

$x_{it}^{in} \in \{0,1\}$	A binary variable that is 1 if ship i begins entering the inbound channel at time t , and 0 otherwise.
$x_{it}^{out} \in \{0,1\}$	A binary variable that is 1 if ship i begins entering the outbound channel at time t , and 0 otherwise.
$y_{it} \in \{0,1\}$	A binary variable that is 1 if ship i occupies pilotage resources at time t , and 0 otherwise.
$z_{it} \in \{0,1\}$	A binary variable that is 1 if ship i occupies tugboat resources at time t , and 0 otherwise.
t_i^{start}	The start time of arrival at the anchorage for ship i .
t_i^{end}	The end time of departure completion for ship i .

234 Secondly, constraints are formulated to reflect the physical and operational limitations within
235 the port, such as berth capacities, waterway traffic restrictions, and resource allocation limits. The
236 objective function of the model is designed to optimize key aspects of port operations, like
237 minimizing total turnaround time, maximizing resource utilization, and ensuring equitable access
238 to port facilities.

239 Objective 1: Maximize the number of ships that have completed the port entry and departure
240 process within the time period T .

241 The objective is formulated as:

$$\text{Maximize } N(T) = \sum_{i \in I} \sum_{t=0}^{T-t_c} x_{it}^{out} \quad (1)$$

242 $N(T)$: The number of ships completing their departure process within the time period T .

243 Objective 2: Minimize the number of auxiliary resources required. The objective is
244 formulated as:

245

$$\text{Minimize } p_{max} = \max_{t \in T} \left(\sum_{i \in I} y_{it} \cdot P_i^{req} + \sum_{i \in I} z_{it} \cdot G_i^{req} \right) \quad (2)$$

246 Objective 3: Minimizing economic costs for single inbound and outbound loading and
247 unloading. The objective is formulated as:

$$\text{Minimize } E = w_{time} \sum_{i \in I} (t_i^{end} - t_i^{start}) + w_{tug} \sum_{i \in I} \sum_{t \in T} (z_{it} \cdot G_i^{req}) \quad (3)$$

248 The weight coefficients w_{time} and w_{tug} were determined based on the actual operational
249 cost data from Tianjin Port. Specifically, they represent the relative monetary value of vessel
250 charter rates per hour versus the hourly service fees for tugboats, ensuring the optimization
251 objective aligns with real-world economic priorities

252 Subject To:

$$\sum_{i \in I} y_{it} \cdot P_i^{req} \leq \|P\|, \forall t \in T \quad (4)$$

$$\sum_{i \in I} z_{it} \cdot G_i^{req} \leq \|G\|, \forall t \in T \quad (5)$$

$$\sum_{i \in I} (\text{ship } i \text{ is at anchorage at time } t) \leq A_{cap}, \forall t \in T \quad (6)$$

$$\sum_{i \in I} (\text{ship } i \text{ is at berth at time } t) \leq B_{cap}, \forall t \in T \quad (7)$$

$$\sum_{i \in I} \sum_{k=0}^{t_c-1} x_{i,t-k}^{in} \leq C_{in}, \forall t \in T \quad (8)$$

$$\sum_{i \in I} \sum_{k=0}^{t_c-1} x_{i,t-k}^{out} \leq C_{out}, \forall t \in T \quad (9)$$

$$x_{it}^{in} \leq y_{i,t+k}, \quad \forall i \in I, \forall t \in T, k = 0, \dots, t_c - 1 \quad (10)$$

$$x_{it}^{in} \leq z_{i,t+k}, \quad \forall i \in I, \forall t \in T, k = 0, \dots, t_c - 1 \quad (11)$$

$$x_{it}^{out} \leq y_{i,t+k}, \quad \forall i \in I, \forall t \in T, k = 0, \dots, t_c - 1 \quad (12)$$

$$x_{it}^{out} \leq z_{i,t+k}, \quad \forall i \in I, \forall t \in T, k = 0, \dots, t_c - 1 \quad (13)$$

253 Where: w_{time} is the cost coefficient for vessel turnaround time, w_{tug} is the cost coefficient for
254 tugboat resource time.

255 Auxiliary Resource Constraints (Eq. 4 & 5): These constraints ensure that at any given time
256 t , the total number of pilots and tugboats in use by all ships does not exceed the total number of
257 available pilots and tugboats, respectively.

258 Capacity Constraints (Eq. 6 to 9): These constraints impose capacity limits on the port's key
259 infrastructure, including the anchorage, berths, inbound channel, and outbound channel, by
260 defining the maximum number of ships that each can accommodate at any given moment.

261 Resource Allocation Logic (Eq. 10 to 13): These are critical logical constraints that link a
262 ship's transit decision to resource utilization. They stipulate that if a ship is scheduled to begin an
263 inbound or outbound transit at time t , the required pilot and tugboat resources must be
264 continuously allocated to that ship for the entire duration of the transit (t_c).

265 Lastly, the model is solved using a combination of simulation and heuristic algorithms,
266 allowing for an efficient and practical approach to managing the complexities of port traffic
267 organisation.

268 4. Solution approach

269 This study employs a SMOGA method which integrates simulation with GA to optimize
270 traffic organisation schemes. It establishes a port navigation system based on CA and MAS. The
271 fitness of multiple optimization objectives in the GA is calculated through simulation.
272 Simultaneously, by setting simulation rules, constraints on various resources are effectively
273 implemented. This approach also allows for the handling of uncertainties in decision variables.

274 4.1 Port navigation simulation model

275 As illustrated in **Fig. 2**, the enhanced simulation model is built upon a dual-layer architecture
276 comprising a physical layer and a logic layer. The **physical layer** represents the tangible
277 components of the port navigation system, including berths, anchorages, channels, and auxiliary
278 pilot and tug services. The **logic layer** governs ship motion through two primary mechanisms: CA
279 update rules for navigation and Multi-Agent information interaction for resource management.
280 Within this logic layer, intelligent agents are assigned to key infrastructure such as anchorages and
281 berths. These agents dynamically monitor and record the occupancy status of their respective
282 components based on real-time operational conditions. Crucially, this agent-based system serves
283 as the practical enforcement mechanism for the conceptual capacity constraints defined in the MIP
284 model as **Eq. (6) and Eq. (7)**. By dynamically approving or denying ship entry requests based on

285 available capacity, the agents ensure these physical limits are strictly observed at the simulation
 286 level. This layer also incorporates a dedicated module to precisely control the deployment of
 287 auxiliary pilot and tug resources. By integrating these control strategies (multi-agent) with
 288 time-spatial discretization (CA), this dual-layer approach provides a comprehensive model of the
 289 port's navigational ecosystem, enabling more effective traffic management and optimization.

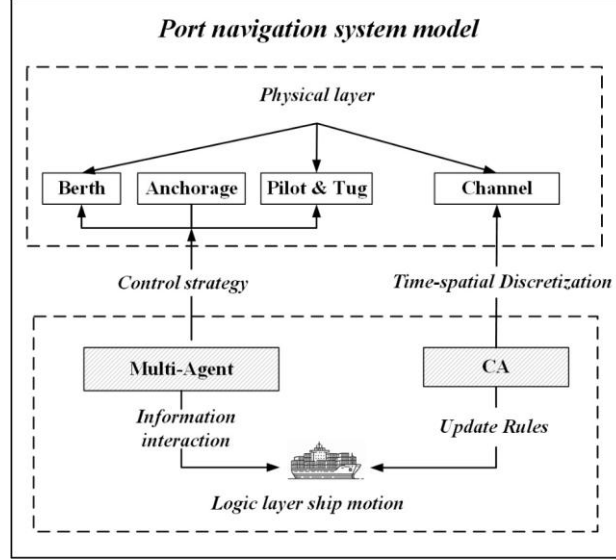


Fig. 2. Structure of simulation model

290
 291
 292
 293

Table 2
Simulation model parameter settings

Indices	
S	All ships.
s_i	Ship i .
$pos(s_i)$	Position of s_i represented as grid coordinates (x, y) .
$S(s_i)$	Status of s_i , include ANCHORAGE, IN_CHANNEL, BERTH, OUT_CHANNEL, COMPLETED.
$type(s_i)$	Type of s_i , $i = 1, 2, 3, \dots, n$.
$res(s_i)$	The resources occupied by s_i , including the number of pilots and tugboats.
C_{space}	The size of the cellular space, (width, height).
V	Mapping of ship type to speed, such as $V[type1] = 2, V[type2] = 1$.

294
 295
 296
 297
 298
 299
 300
 301
 302
 303

1) Acceleration
 Let a be the acceleration and v_t be the velocity at time t , $pos_t(s_i) = (x_t, y_t)$ be the position of ship s_i at time t . Then the calculation of acceleration can be expressed as Eq. (14).

$$v_{t+1}(s_i) = v_t(s_i) + a \quad (14)$$

2) Deceleration/Collision Avoidance
 If another ship or obstacle is detected ahead, slow down or stop to avoid a collision. Assuming d is the distance between the two ships and v_t is the current speed, the deceleration can be expressed as Eq. (15).

$$v_{t+1}(s_i) = \begin{cases} 0 & \text{if } d \leq \text{safety distance} \\ v_t(s_i) & \text{otherwise} \end{cases} \quad (15)$$

3) Position Update
 Let (x_t, y_t) be the position at time t , and v_t be the velocity. Position updates can be calculated based on Eq. (16).

$$pos_{t+1}(s_i) = (x_t, y_t + v_{t+1}(s_i)) \quad (16)$$

304 4) Resource Control

305 R is the total number of resources, depending on G and P , The occupation of resources can
 306 be expressed by Eq. (17).

$$R_{t+1} = R_t - r_{required} \text{ if } R_t \geq r_{required} \quad (17)$$

307 Resource release can be expressed in Eq. (18).

$$R_{t+1} = R_t + r_{released} \quad (18)$$

308 5) Status Update

309 The state transitions for ships in the simulation model follow the rules below. The symbols
 310 for the transition conditions are defined as follows:

311 C_1 : A berth has been assigned to the ship.

312 C_2 : The required auxiliary resources (pilots, tugs) for the transit are available.

313 C_3 : The ship has reached its assigned berth position.

314 C_4 : The ship's port service is complete.

315 C_5 : The ship has left the designated port waterway area.

316 a. From ANCHORAGE to IN_CHANNEL (from anchorage to inbound channel)

$$S_{t+1}(s_i) = \begin{cases} \text{IN_CHANNEL}, & \text{if } S_t(s_i) = \text{ANCHORAGE} \wedge C_1 \wedge C_2 \\ S_t(s_i) & \text{otherwise} \end{cases} \quad (19)$$

317 b. From IN_CHANNEL to BERTH (from inbound channel to berth):

$$S_{t+1}(s_i) = \begin{cases} \text{BERTH}, & \text{if } S_t(s_i) = \text{IN_CHANNEL} \wedge C_3 \\ S_t(s_i) & \text{otherwise} \end{cases} \quad (20)$$

318 c. From BERTH to OUT_CHANNEL (from berth to outbound channel):

$$S_{t+1}(s_i) = \begin{cases} \text{OUT_CHANNEL}, & \text{if } S_t(s_i) = \text{BERTH} \wedge C_4 \wedge C_2 \\ S_t(s_i) & \text{otherwise} \end{cases} \quad (21)$$

319 d. From OUT_CHANNEL to COMPLETED (from outbound channel to completed status):

$$S_{t+1}(s_i) = \begin{cases} \text{COMPLETED} & \text{if } S_t(s_i) = \text{OUT_CHANNEL} \wedge C_5 \\ S_t(s_i) & \text{otherwise} \end{cases} \quad (22)$$

320 In the optimization of traffic organisation of the port navigation system, there are
 321 uncertainties in the transformation of ship status and ship navigation. The resource control and
 322 ship status conversion in the study are controlled by a MAS. The uncertainty in traffic organisation
 323 optimization can be expressed as Eq. (23):

$$S_{t+1} = f(S_t, X_t, R_t, M_t), \text{ where } M_t \sim \mathcal{N}(0, \sigma^2) \quad (23)$$

324 S_t is the ship state at time t .

325 X_t is the port resource availability at time t , such as berths and channels.

326 R_t is the availability of auxiliary resources at time t , such as tugs, pilots.

327 M_t is a random variable, representing uncertainty factors, such as changes in ship motion,
 328 etc.

329 In this study, the movement of ships is governed by the fundamental rules of CA (Eq. 14-16),
 330 while their interactions are managed in real-time by the multi-agent module. To explicitly model
 331 the ‘‘Local Interaction’’ and ‘‘Cooperative Autonomy’’ of the system, specific communication
 332 logics are integrated:

333 1. Collision Avoidance (Micro-level): Based on Eq. (15), when a following ship detects that
 334 the distance to the preceding ship is less than the safety threshold, it autonomously triggers a
 335 deceleration mechanism. This simulates the localized perception-reaction loop essential for
 336 autonomous navigation.

337 2. Resource Negotiation (Macro-level): Unlike static scheduling where conflicts lead to
 338 infeasible solutions, the MAS possesses adaptive self-correction capabilities. When a ship requests
 339 entry, the Berth and Channel Agents autonomously evaluate real-time capacity (Eq. 6-9). If

340 resources are fully occupied or stochastic disruptions occur (Eq. 23), the agents execute a
 341 “Refusal-and-Wait” logic: they deny the request (Eq. 17) and return a “Wait” signal,
 342 compelling the Ship Agent to autonomously transition to the anchorage waiting state (Eq. 19).
 343 This decentralized negotiation ensures that global schedules remain robust against dynamic
 344 uncertainties without human intervention.

345 Furthermore, the simulation model performs a dual role beyond mere validation. Crucially, it
 346 serves as the Dynamic Fitness Evaluator within the SMOGA optimization loop. By subjecting
 347 each candidate schedule to these stochastic environmental constraints, the Digital Twin allows the
 348 optimizer to 'perceive' the non-linear impact of random disruptions, identifying robust solutions
 349 that static mathematical models would overlook.

350 4.2 Simulation-based Multi-Objective Genetic Algorithm (SMOGA)

351 Considering the fact that different types of ships have varying speeds for loading and
 352 unloading, navigation, as well as distinct auxiliary resource requirements, the sequencing of ships,
 353 along with their waiting times at berths and durations at anchorages, plays a pivotal role in
 354 influencing traffic efficiency. This study focuses on the sequencing of an array of ship types and
 355 their dwell times at different locations as key decision variables. These variables are subjected to
 356 mutation and crossover processes, with the resultant variations forming the basis of traffic
 357 organisation plans. These plans are then integrated into the simulation module, where the fitness
 358 of each plan is assessed based on the outcomes of the simulation. Resource constraints are
 359 enforced through simulation rules, and adjustments in ship status are made to effectively manage
 360 uncertainties. The optimization objectives are to **minimize** the required auxiliary resources,
 361 **maximize** the ship throughput, and **reduce** the average completion time. This approach
 362 culminates in the creation of a SMOGA framework, which incorporates simulation to address the
 363 multi-objective optimization challenges inherent in traffic organisation plans. The logic of this
 364 solution framework is depicted in **Algorithm 1**.

Algorithm 1. SMOGA for Ship Traffic Optimization

Input:

P_{size} : Size of the population
 G_{max} : Number of generations for evolution
 D_{sim} : Generate the initial population

Output:

\mathcal{P}^* : The Pareto-optimal set of solutions

	Procedure:
1	// Initialization
2	$t \leftarrow 0$
3	$\mathcal{P}_0 \leftarrow \text{InitializePopulation}(D_{sim}, P_{size})$
4	// Main Evolutionary Loop
5	WHILE $t < G_{max}$
6	// Fitness Calculation
7	FOR EACH individual plan $\pi \in \mathcal{P}_t$ DO
8	$[N(\pi), p_{max}(\pi), T_{avg}(\pi)] \leftarrow \text{Simulation}(\pi)$
9	// Fitness vector for minimization: (-Completed Ships, Peak Resources, Avg Completion
10	Time)
11	$F(\pi) \leftarrow (-N(\pi), p_{max}(\pi), T_{avg}(\pi))$
12	END FOR
13	// Elite Selection (NSGA-II Strategy)
14	$\mathcal{F} \leftarrow \text{FastNonDominatedSort}(\mathcal{P}_t)$
15	$\mathcal{P}_{t+1} \leftarrow \mathcal{F}$
	$i \leftarrow 1$

```

16      WHILE  $|\mathcal{P}_{t+1}| + |\mathcal{F}_i| \leq P_{size}$  DO
17          Crowding Distance Assignment ( $\mathcal{F}_i$ )
18           $\mathcal{P}_{t+1} \leftarrow \mathcal{P}_{t+1} \cup \mathcal{F}_i$ 
19           $i \leftarrow i + 1$ 
20      END WHILE
21      Sort ( $\mathcal{F}_i, crowding\_distance$ )
22       $\mathcal{P}_{t+1} \leftarrow \mathcal{P}_{t+1} \cup \mathcal{F}_i[1:(P_{size} - |\mathcal{P}_{t+1}|)]$ 
23      // Offspring Generation
24       $Q_{t+1} \leftarrow Generate\ Offspring(\mathcal{P}_{t+1}, Crossover, Mutation)$ 
25       $\mathcal{P}_t = Q_{t+1}$ 
26       $t \leftarrow t + 1$ 
27      END WHILE
28      // Return the first Pareto front
29       $\mathcal{P}^* \leftarrow FastNonDominatedSort(\mathcal{P}_t)[0]$ 
30      RETURN  $\mathcal{P}^*$ 

```

365 1) Fitness Calculation

366 The calculation of fitness is a crucial step for selecting the optimal offspring within a
367 population. In this study, the traditional mathematical approach to fitness calculation has been
368 supplanted by a simulation-based method. This involves evaluating offspring based on the number
369 of ships that successfully pass through, the required maximum number of p_{max} , and the average
370 completion time, thereby allowing for a comprehensive assessment.

371 2) Constraints

372 Constraints play an important role in optimization algorithms. This research primarily
373 incorporates two types of constraints: ship movement constraints and resource constraints. Ship
374 movement constraints are enforced through the ship position update rules within the simulation
375 model. Resource constraints are dynamically determined by the control modules of the MAS
376 within the simulation model.

377 3) Crossover Strategy

378 The crossover strategy is a key operator in GA to generate new individuals, aiming to
379 combine characteristics from two parent individuals to produce new offspring. The specific steps
380 include:

381 Offspring Initialization: Two entirely independent offspring are created from two parent
382 individuals, retaining all characteristics of the parents. This step is accomplished through deep
383 copying to ensure that the offspring's operations do not affect the parents.

384 Attribute Exchange: For each ship, the algorithm searches for potential exchange candidates
385 at the corresponding positions in the parent individuals. This search is confined to a specific range
386 around each ship (i.e., the range of n ships ahead and behind).

387 The type determination and exchange logic are reflected in Formula (24): If two ships are of
388 different types, their arrival times and anchorage waiting times are exchanged. If they are of the
389 same type, then their berth waiting times are swapped. This step considers the characteristic
390 differences between different types of ships and promotes genetic diversity while preserving type
391 characteristics.

$$\begin{aligned}
& C_1[i], C_2[i] \\
& = \begin{cases} \text{swap}(P_1[i], P_2[i], \text{arrival_time}, \text{anchorage_waiting_time}) & \text{if } P_1[i].\text{type} \neq P_2[i].\text{type} \\ \text{swap}(P_1[i], P_2[i], \text{berth_waiting_time}) & \text{otherwise} \end{cases} \quad (24)
\end{aligned}$$

392 4) Mutation Strategy

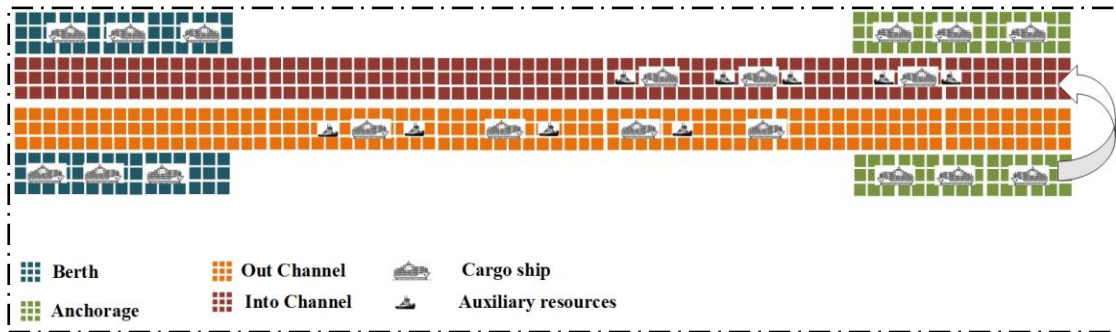
393 The mutation strategy in GA is a critical mechanism for introducing new characteristics and
394 increasing population diversity. Initially, an individual is copied to avoid direct modifications to
395 the original, ensuring the independence of the mutation operation. For each ship, a decision is

396 made on whether to mutate based on a pre-set mutation rate. This step ensures that the mutation is
 397 not over-applied in each generation, thereby maintaining a balance between exploration and
 398 exploitation. The minimum waiting time at the berth is determined based on the ship type, as well
 399 as the corresponding mutation value, and adjustments are made to the waiting times at anchorage
 400 and berth accordingly. Particularly for the mutation of arrival times, it is also necessary to ensure
 401 that the mutated time does not overlap with the arrival times of other ships, maintaining
 402 uniqueness in timing (as indicated in Eq. (25)).

$$\begin{aligned}
 \text{data[anchorage waiting time]} &= \max(0, \text{ship_data[anchorage_waiting_time]} \\
 &+ \text{variation}) \text{ship_data[berth_waiting_time]} \\
 &= \max(\text{berth_waiting_time_min}, \text{ship_data[berth_waiting_time]} \\
 &+ \text{variation})
 \end{aligned} \tag{25}$$

403 5. Case study

404 In this study, the main channel of Tianjin Port and its corresponding port area have been
 405 selected as the case study. The setting of relevant parameters is based on port information and ship
 406 AIS data, and **Fig. 3** illustrates the effect of the port space after discretization. Regarding
 407 parameter settings, consistent with the current port area of Tianjin Port's main channel, 15 berths
 408 have been established. Ship types are categorized into three classes (50,000 tons, 70,000 tons, and
 409 100,000 tons), with speeds determined based on data extracted from AIS records. **Table 3** displays
 410 the detailed parameter settings, in which the speed strategy adopts previous related research (Liu
 411 et al., 2024b). These settings include the specific dimensions and capacities of the berths, the
 412 designated types and quantities of the ships, and the operational speeds derived from real-world
 413 navigational data. This careful calibration of parameters ensures that the simulation model closely
 414 mirrors the actual conditions and operational practices of Tianjin Port, providing a realistic and
 415 robust basis for the subsequent optimization processes. The model considers the dynamic and
 416 stochastic nature of port operations, including variations in arrival times, service durations, and the
 417 availability of key resources such as tugs and pilots.



419 **Fig. 3.** Simulation space discretization diagram

420 **Table 3**

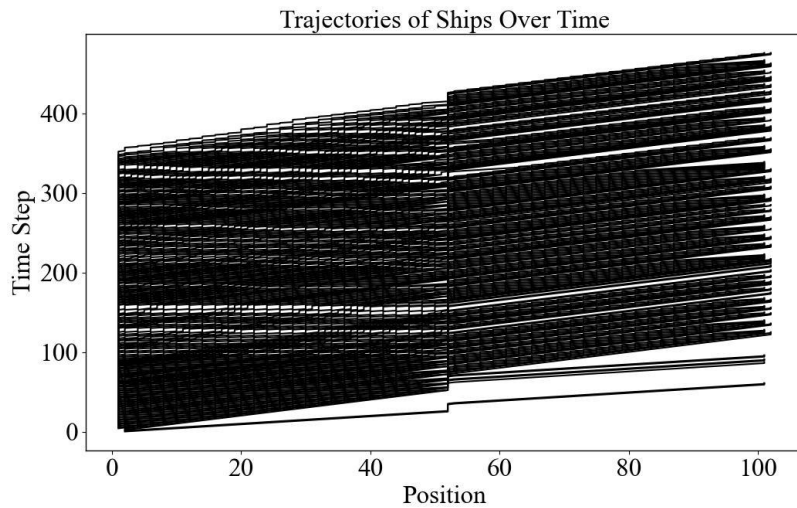
421 Ship parameters

Ship type	Required assistant resources	Unloading time (hour)	Speed strategy
Type 1	1	10	1
Type 2	2	15	2
Type 3	2	20	3

422 5.1 Validation of simulation model

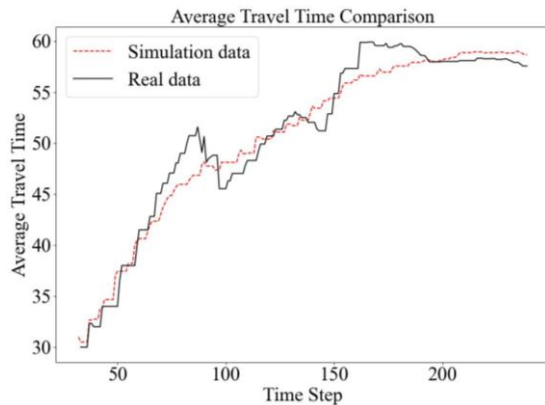
423 An observation of the experimental results reveals a notable alignment of ship trajectories
 424 with those predicted by the CA-based traffic simulation (shown in **Fig. 4**). A key finding is that the
 425 average time taken for ships to complete their voyages gradually stabilises over time (shown in
 426 **Fig. 5**). Furthermore, the number of ships completing their entry and exit voyages from the port
 427 incrementally increases as time progresses (refer to **Fig. 6**).

428 This progression is corroborated by the recorded fluctuations in the time taken for each ship
 429 to complete its voyage. These fluctuations align consistently with the statistical results of the
 430 average completion time for ships, as depicted in **Fig. 7**. The Mean Absolute Error (MAE) for the
 431 average completion time stands at 1.312. Furthermore, the MAE for the number of ships
 432 completing their voyages is 1.870, indicating a strong correspondence with the actual AIS data,
 433 thereby validating the reliability of our model. The simulation results also demonstrate that the
 434 occupancy rates of each resource vary with time steps, aligning with the operational patterns of the
 435 port navigation system. This variation in resource utilisation, in tandem with the correlated data on
 436 ship completion times and numbers, provides a comprehensive insight into the dynamics of port
 437 operations (shown in **Fig. 8**). These experimental outcomes and their subsequent analysis
 438 substantiate the rationality and efficacy of the simulation model. The coherence between the
 439 observed results and the expected patterns of port traffic behaviour provides compelling evidence
 440 of the model's validity.



441
 442

Fig. 4. Ship trajectory from simulation results



443

Fig. 5. Comparison of average completion

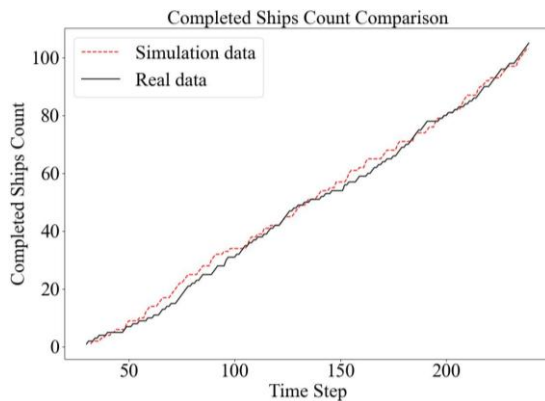
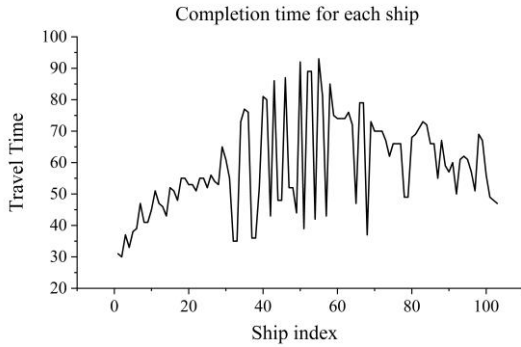
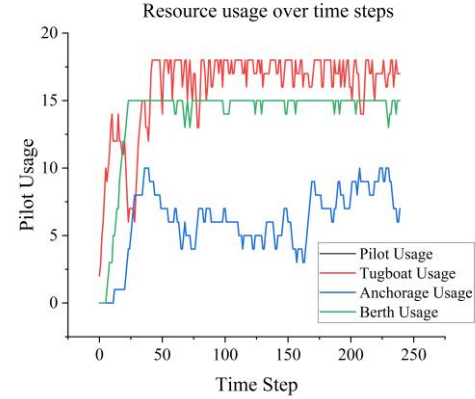


Fig. 6. Comparison of the number of

time between real data and simulated data



completed ships between real data and simulated data



444

Fig. 7. Average completion time variation of simulation data

Fig. 8. Simulated port resource occupancy

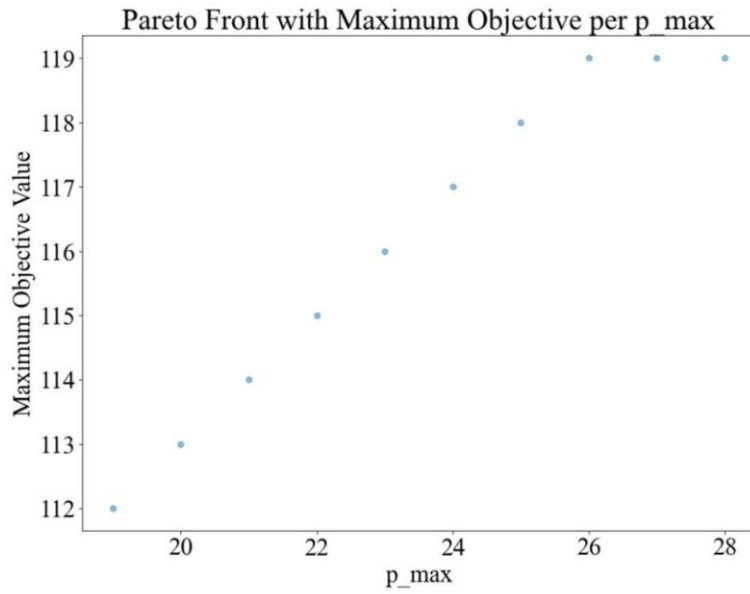
445 5.2 Simulation-based multi-objective Genetic Algorithm (SMOGA) optimization

446 experiment

447 The benchmark scheme compared in this study is FCFS (First-Come, First-Served)
448 scheduling, and resources are allocated according to demand. For heuristic optimization
449 algorithms, each additional optimization objective adds to the computational difficulty and slows
450 down the search for optimal solutions. Therefore, three multi-objective optimization problems
451 were designed in this study. The first problem aims to minimize p_{max} and maximize N ,
452 conducting multi-objective optimization to find the traffic organisation plan that achieves the
453 maximum number of ship completions within time T under different max configurations. The
454 second problem considers not only p_{max} and N , but also adds an objective of minimising the
455 average completion time of ships. The first problem considers only the optimal results for the
456 maximum number of completed ships within time T in relation to p_{max} , while the second
457 problem, in addition to considering the maximum number of ships that complete navigation, also
458 considers the average completion time of the ships. Building upon the foundation of the previous
459 two problems, we consider the economic indicator E during the process of ships entering and
460 exiting ports, forming a third problem. The E is influenced by both T and p_{max} .

461 5.2.1 Problem 1: Optimization experiments by maximum number of ships

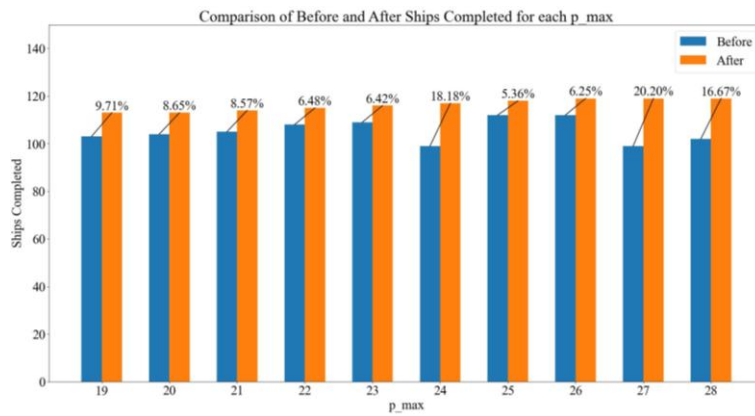
462 For port managers, determining the arrival time, anchoring time, time of entry into the
463 channel, and time of departure from the berth for each ship enables effective autonomous
464 scheduling and management. The information for all ships over a period collectively forms a set of
465 traffic organisation plans. Using the simulation model, traffic organisation plans generated from
466 50 runs under pre-set parameters serve as the initial population. Each traffic organisation plan
467 includes the ship's ID, arrival time, anchorage time, and berth waiting time. Iterative optimization
468 is conducted on two objectives: minimizing the quantity of p_{max} and the number of ships
469 completing navigation. The variation of optimization objectives with the number of iterations
470 under different p_{max} is recorded, resulting in the outcomes depicted in **Fig. 9**.



471

472

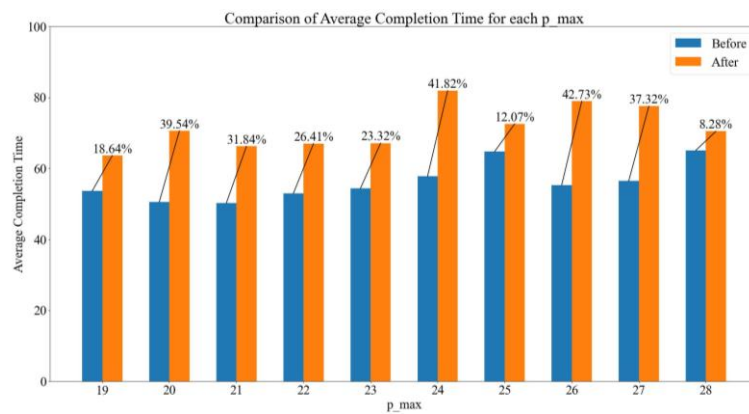
(a)



473

474

(b)



475

476

(c)

477

478

479

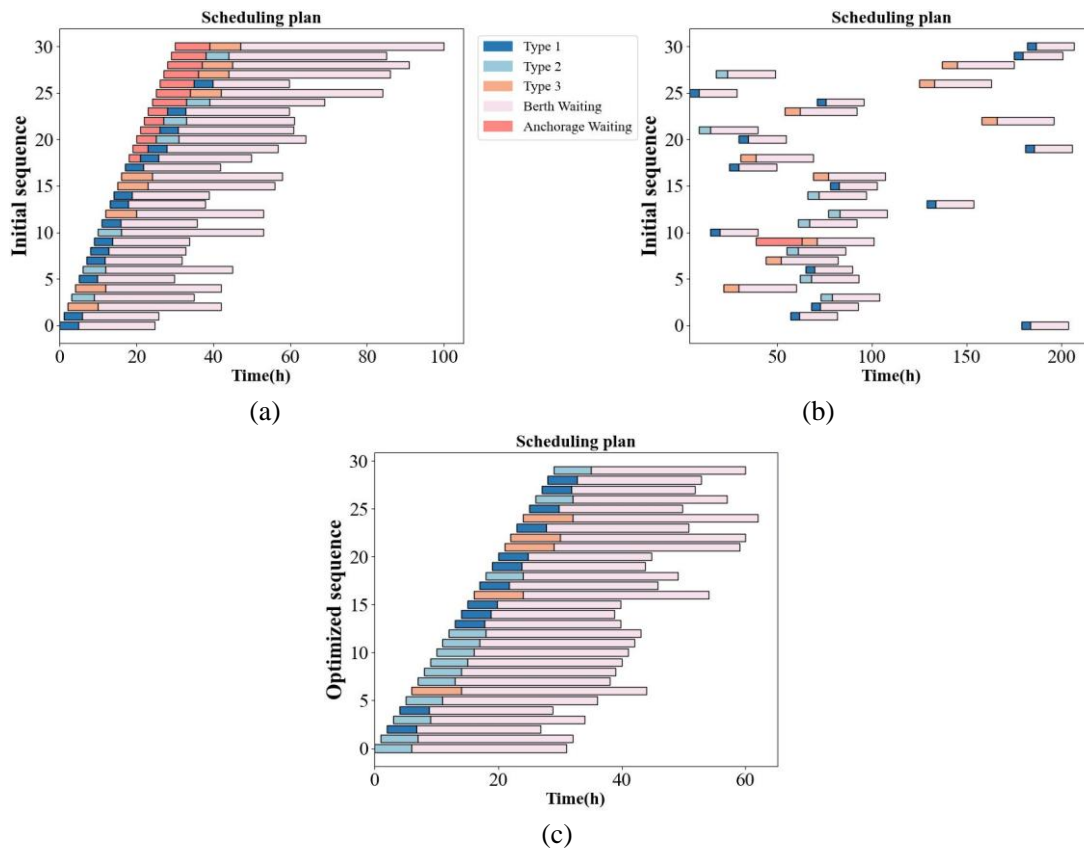
Fig. 9. Experiment result for problem 1: (a) Pareto front with maximum ships completed per p_{max} , (b) Comparison of the number of completed ships before and after optimization, (c) Comparison of the average time for ships to complete their voyage before and after optimization.

480 The experimental results show that for **Fig. 9 (a)**, the Pareto front formed by the two
 481 optimization objectives represents traffic organisation plans optimized for each point, recording
 482 the Pareto front of the number of ships completing entry and exit from the port as auxiliary
 483 resources vary.

484 b. A comparison between two sets of traffic organisation plans before and after optimization
 485 clearly reveals that the number of ships completed after optimization increased by varying
 486 amounts, ranging from 5.36% to 20.20% (**Fig. 9 (b)**), while the average completion time for ships
 487 entering and leaving the port increased by 12.07% to 42.73% (**Fig. 9 (c)**).

488 c. It can be seen that the optimization effect is mainly reflected in reducing waiting time at
 489 the anchorage by adjusting the order of ships, thereby achieving the effect of optimizing efficiency,
 490 as illustrated in **Fig. 10**.

491



492

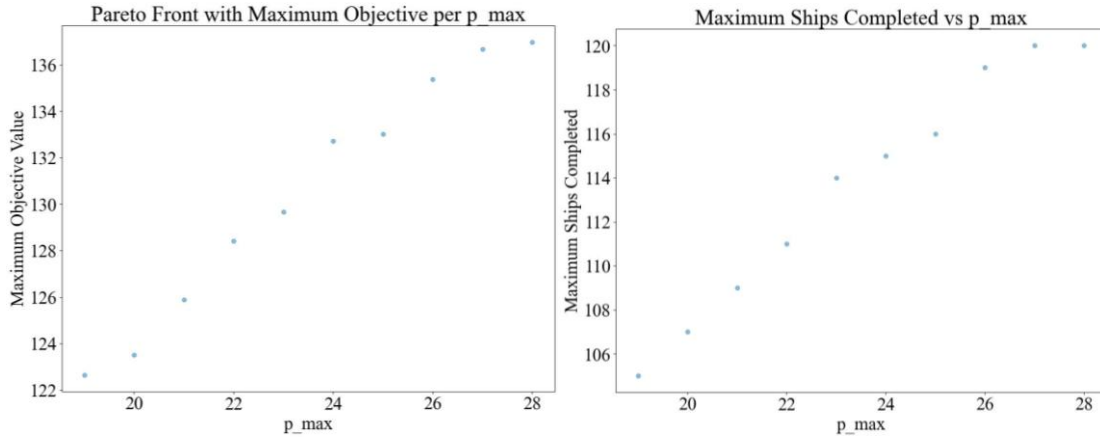
493

494

495 **Fig. 10.** Visualization of scheduling plan before and after autonomous optimization of problem 1:
 496 (a) Initial scheduling plan for the first 30 ships, (b) Optimized scheduling plan for the original first
 497 30 ships, (c) Optimized scheduling plan for the new first 30 ships

498 **5.2.2 Problem 2: Optimization experiments considering minimum average ship passage time**
 499 **and maximum number of ships**

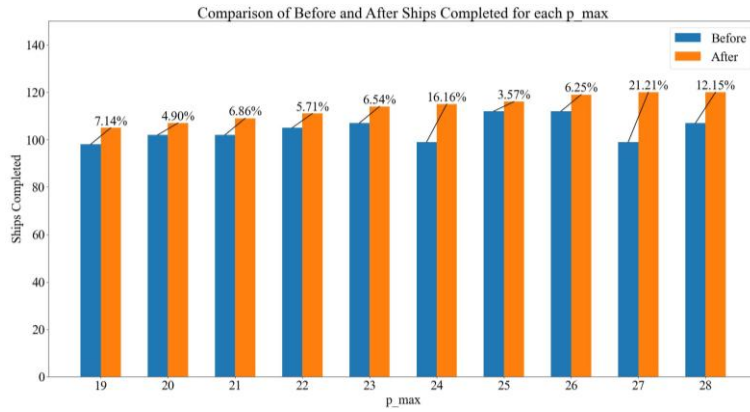
500 Iterative optimization was performed on the three objectives: minimizing the quantity of
 501 p_{max} , maximizing the number of ships completing navigation, and minimizing the average ship
 502 passage time. The changes in the optimization objectives under different p_{max} values were
 503 recorded throughout the iteration process. The results obtained are displayed in **Fig. 11**. These
 504 figures illustrate the trajectories of optimization progress, reflecting how the solutions evolve over
 505 time with respect to the number of auxiliary resources p_{max} and the composite objective function.



506

(a)

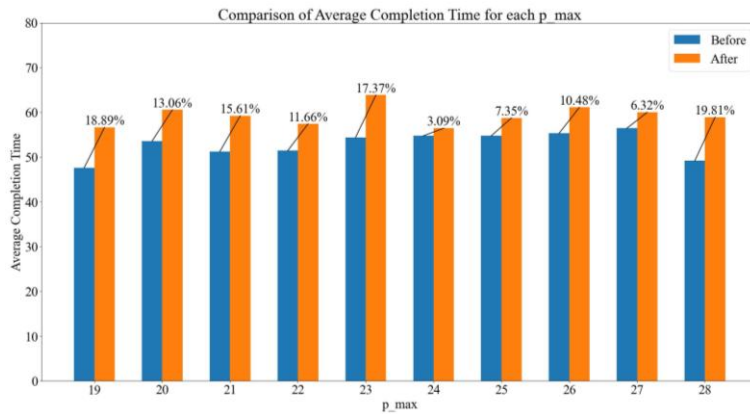
(b)



507

508

(c)



509

510

(d)

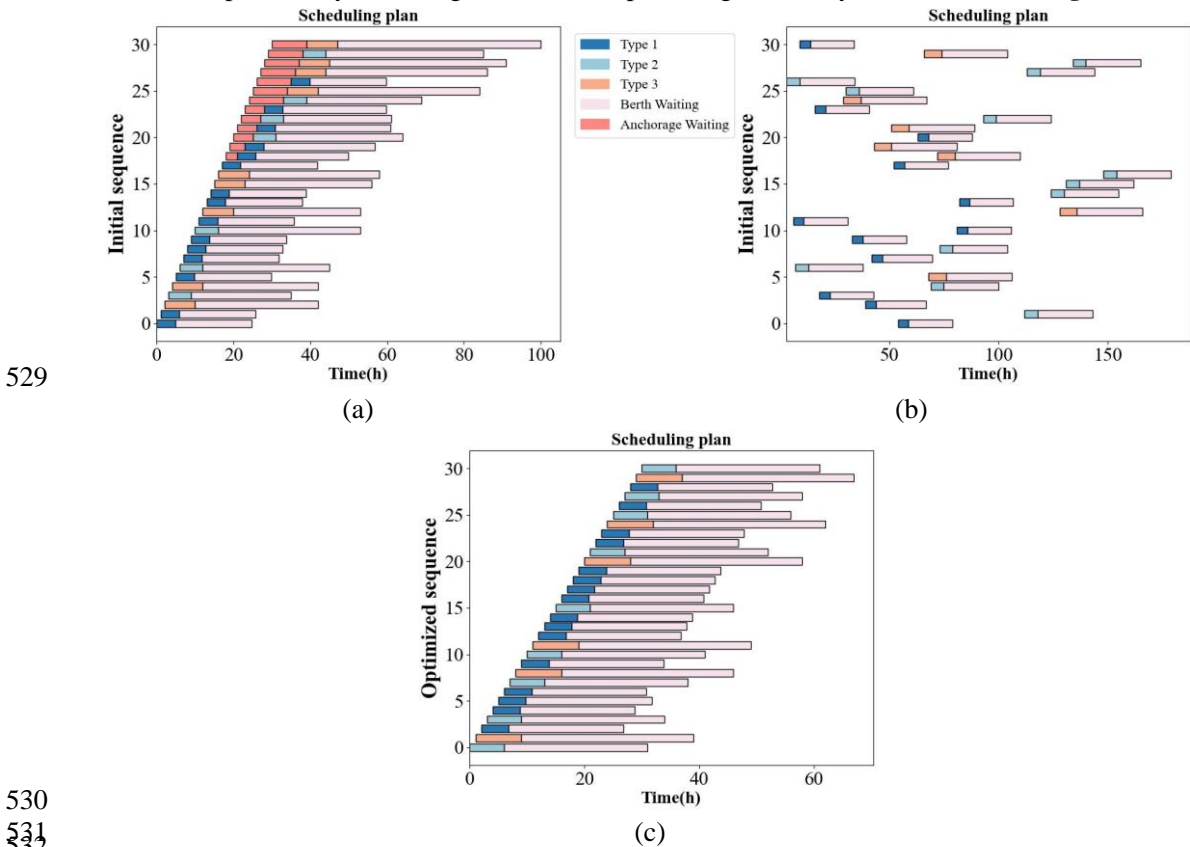
511 **Fig. 11.** Experiment result for problem 2: Pareto front:(a) maximum objective per p_{max} , (b)
 512 maximum ships completed per p_{max} , Comparison: (c) the number of completed ships before and
 513 after optimization, (d) the average time for ships to complete their voyage before and after
 514 optimization

515 a. After incorporating consideration for the average completion time, it is observed that the
 516 optimization results still ensure that the trends of the maximum number of ships passing and the
 517 objective function remain consistent (**Fig. 11(a)**). Ultimately, it is still possible to obtain a traffic
 518 organisation plan that accommodates the maximum number of ships (**Fig. 11(b)**).

519 b. As the average completion time is considered, the traffic organisation plans optimized
 520 subsequently do not exhibit a significant increase in the average completion time of ships, unlike
 521 in problem 1 (**Fig. 9**).

522 c. It is evident that with the variation in the required maximum number of auxiliary resources
 523 p_{max} , the number of ships completed after optimization increased by 4.9% to 21.21% (**Fig. 11(c)**),
 524 but the average completion time for ships entering and leaving the port increased by only 3.09% to
 525 19.81% (**Fig. 11(d)**).

526 d. It can be seen that the optimization approach and effect are the same as in problem 1, the
 527 optimization effect is mainly reflected in reducing waiting time at the anchorage by adjusting the
 528 order of ships, thereby achieving the effect of optimizing efficiency, as illustrated in **Fig. 12**.



530

531

532

533

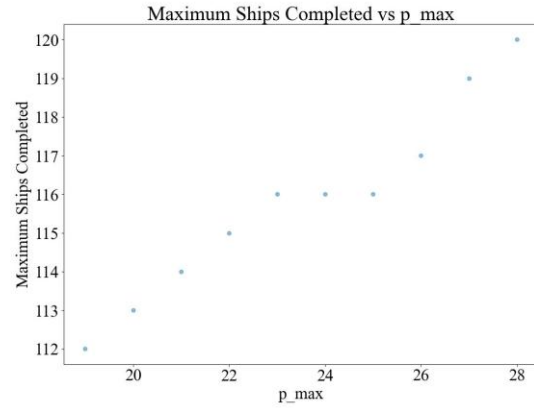
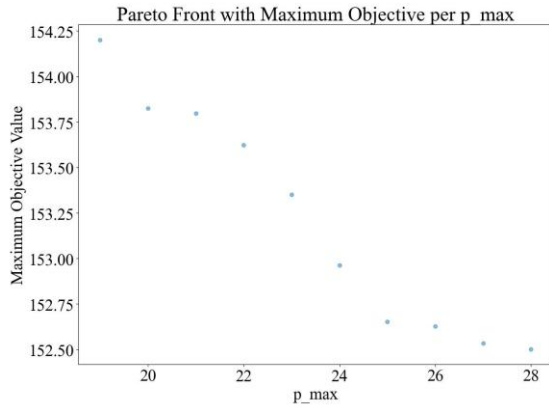
534

535

Fig. 12. Visualization of scheduling plan before and after optimization of problem 2: (a) Initial scheduling plan for the first 30 ships, (b) Optimized autonomous scheduling plan for the original first 30 ships, (c) Optimized autonomous scheduling plan for the new first 30 ships

536 **5.2.3 Problem 3: Optimization experiments considering minimum average ship passage time,**
 537 **maximum number of ships and economic cost**

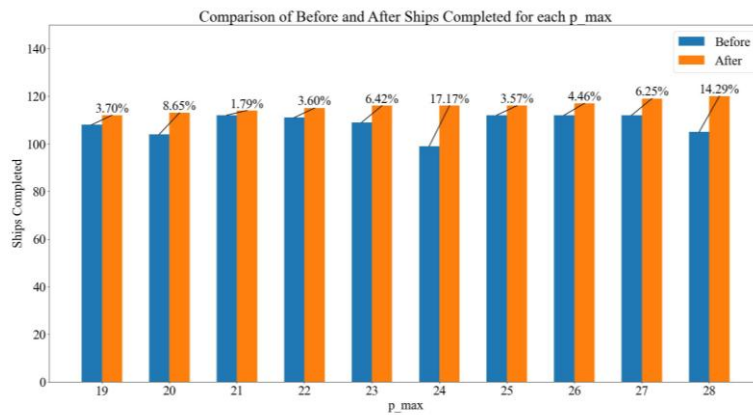
538 The economic efficiency of a ship during its entry and exit process is influenced by the
 539 resources used, denoted as p_{max} , and the average time taken for a single ship to complete the
 540 entry and exit. The longer the time spent on these resources, the longer the average time for entry
 541 and exit, resulting in a higher value for the economic index E , which signifies poorer economic
 542 efficiency. Therefore, after incorporating the economic efficiency index into the weighted
 543 objectives, new experimental results were obtained.



544

(a)

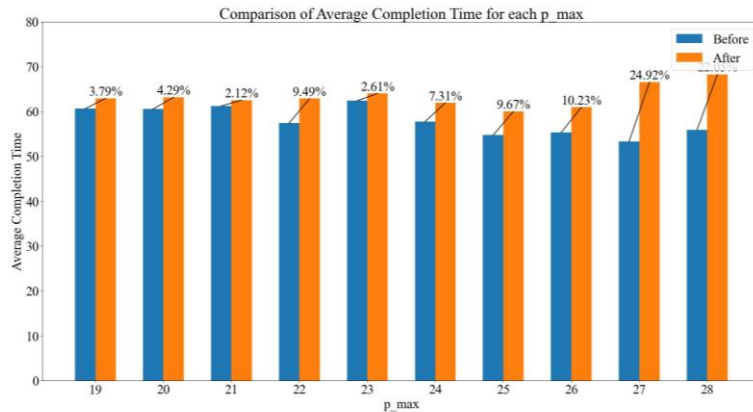
(b)



545

546

(c)



547

548

(d)

549 **Fig. 13.** Experiment result for problem 3: Pareto front:(a) maximum objective per p_{max}
 550 considering economic cost, (b) maximum ships completed per p_{max} considering economic cost,
 551 Comparison: (c) the number of completed ships before and after optimization considering
 552 economic cost, (d) the average time for ships to complete their voyage before and after
 553 optimization considering economic cost

554

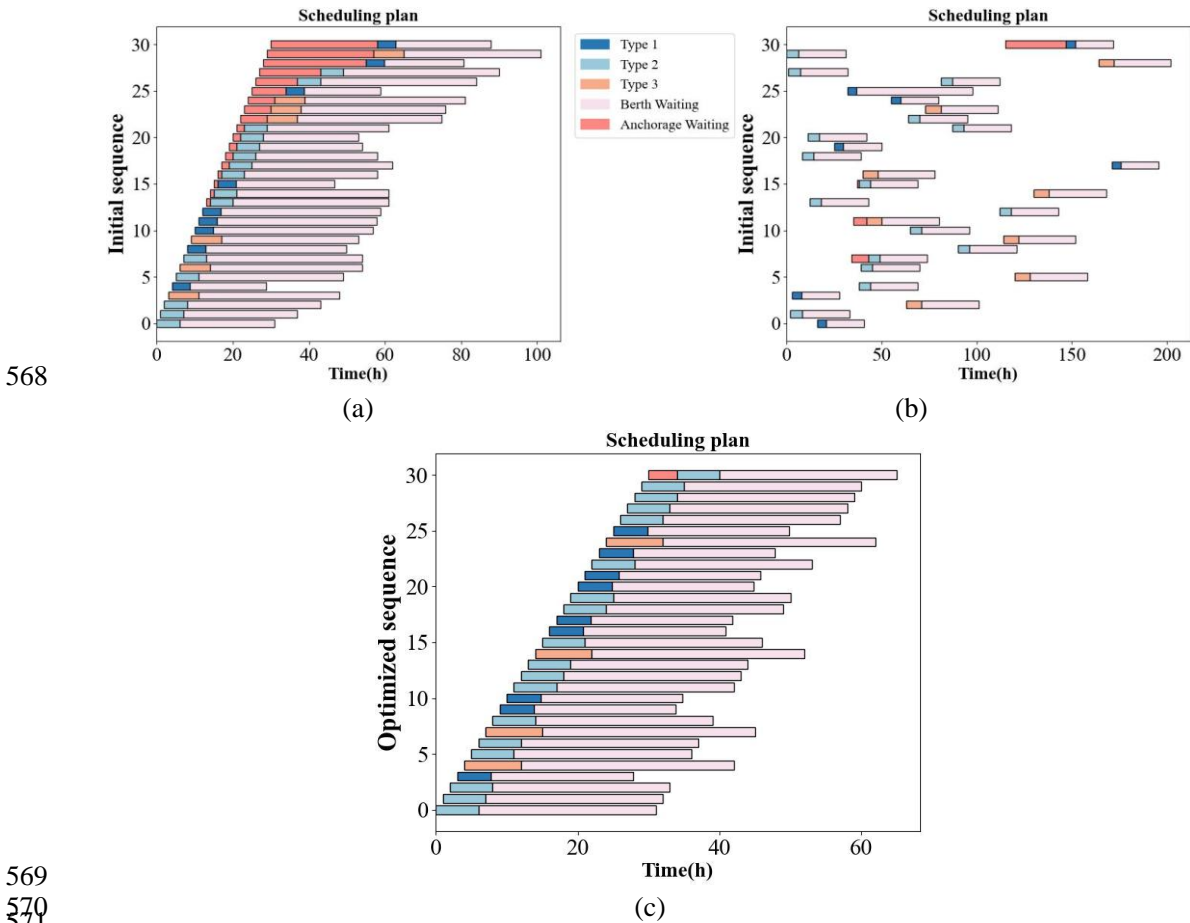
a. From **Fig. 13(a)**, it can be observed that, unlike problem 1 and problem 2, the weighted

555 objective value shows an inversely proportional trend with the increase of p_{max} .

556 b. As can be observed from **Fig. 13(b)**, the proposed algorithm framework is still able to
 557 generate traffic organisation schemes corresponding to different maximum completion ship
 558 quantities (p_{max}), even after considering economic factors. Moreover, this quantity increases with
 559 the increase of p_{max} .

560 c. Analysis of the results before and after optimization reveals that (**Fig. 13(c)**, **Fig. 13(d)**), in
 561 terms of the number of ships optimized for navigation completion, there is no obvious trend for
 562 different p_{max} optimization effects. However, in terms of average completion time, as p_{max}
 563 increases, the average time for ships to complete navigation increases more significantly.

564 d. The experimental results indicate that after taking economic factors into account, the
 565 optimization effect is still evident. This is achieved by reordering the sequence of ships,
 566 effectively reducing the waiting time of ships at anchorages, thereby enhancing traffic efficiency,
 567 as illustrated in **Fig. 14**.



568

569

570

571

572

573

574

575

576

577

578

579

580

Fig. 14. Visualization of scheduling plan before and after optimization of problem 3: (a) Initial scheduling plan for the first 30 ships, (b) Optimized autonomous scheduling plan for the original first 30 ships, (c) Optimized autonomous scheduling plan for the new first 30 ships

5.3 Benchmark analysis and algorithm validating

To rigorously validate the performance of the proposed SMOGA, a comprehensive comparative study was conducted. In addition to the baseline First-Come, First-Served (FCFS) rule and standard meta-heuristics like NSGA-II and Particle Swarm Optimization (PSO), we expanded the benchmark to include Ant Colony Optimization (ACO), Simulated Annealing (SA), and the Grey Wolf Optimizer (GWO), which has demonstrated superior performance in recent

581 path planning studies. To ensure fair comparison, the basic parameters of all algorithms were
 582 standardized: the population size was set to 50, and the maximum number of iterations was set to
 583 100, consistent with the proposed SMOGA algorithm. For algorithm-specific parameters (e.g.,
 584 crossover/mutation rate of NSGA-II, inertia weight of PSO), we adopted common configurations
 585 and verified their convergence through preliminary tuning experiments.

586 All algorithms were tested across the three defined problems to evaluate their capabilities in
 587 terms of port throughput (number of completed ships) and operational efficiency (average
 588 turnaround time). The comparative results are summarized in Table 4 and visualized in Fig. 15.
 589 Table 4. Performance comparison of SMOGA with benchmark algorithms.

Scenarios	Algorithms	Number of completed ships after optimization	Average time for ships to complete their voyage after optimization
Problem 1	FCFS	103	53.65
	NSGA-II	115	80.27
	PSO	110	75.34
	ACO	108	72.80
	SA	110	74.37
	GWO	111	77.92
	SMOGA	119	70.47
Problem 2:	FCFS	103	53.65
	NSGA-II	116	66.78
	PSO	111	65.33
	ACO	108	60.62
	SA	112	73.63
	GWO	113	74.18
	SMOGA	120	58.94
Problem 3	FCFS	103	53.65
	NSGA-II	115	78.36
	PSO	110	74.29
	ACO	112	72.80
	SA	110	74.37
	GWO	114	76.46
	SMOGA	120	68.28

590 The comparative results in Table 4 and Fig. 15 demonstrate the comprehensive superiority of
 591 the proposed SMOGA framework:

592 1. Dominance in Throughput: SMOGA consistently achieves the highest port capacity. In
 593 Problem 2, for instance, SMOGA successfully scheduled 120 ships, significantly outperforming
 594 the best alternative meta-heuristics, GWO (113 ships) and SA (112 ships). Traditional algorithms
 595 like ACO lagged further behind (108 ships), proving that the proposed simulation-based
 596 mechanism explores the solution space more effectively than standard swarm intelligence.

597 2. Superior Efficiency (Strict Dominance): A striking finding from the updated data is that
 598 SMOGA is the most efficient among all optimization algorithms.

599 Beating the Swarm: While algorithms like GWO and ACO are often cited for their speed, in
 600 this complex constraint environment, they incurred higher average delays. For example, in
 601 Problem 2, the average completion times for ACO (60.62h) and GWO (74.18h) were notably

602 higher than that of SMOGA (58.94h).

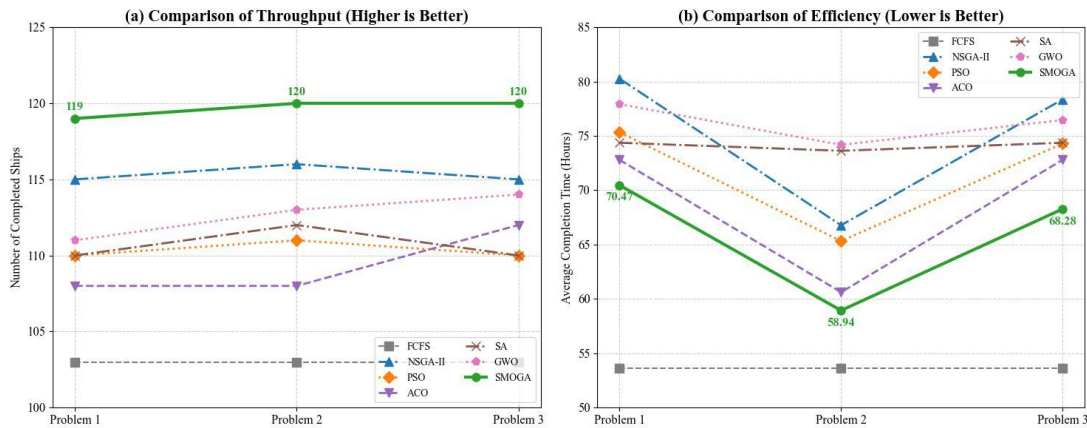
603 The Only Outlier: The only method faster than SMOGA is the baseline FCFS (53.65h).
 604 However, this speed is deceptive, as FCFS achieves it by simply failing to schedule nearly 15% of
 605 the vessels (only 103 completed).

606 To provide a comprehensive evaluation beyond numerical results, Table 5 presents a
 607 qualitative comparison of the proposed SMOGA against mainstream port scheduling approaches
 608 across four key dimensions: data fusion capability, handling of stochastic randomness, support for
 609 autonomous behaviors, and computational balance.

610 Table 5. Qualitative comparison of different scheduling frameworks.

Feature Framework	Rule-based (FCFS)	Traditional MIP	Standard Meta-heuristics (NSGA-II/PSO)	Proposed SMOGA
Multi-source Data Fusion	Low (Single source)	Medium (Static constraints)	Medium (Penalty functions)	High (MIP + Digital Twin Integration)
Stochastic Randomness	None (Deterministic)	Low (Hard to solve)	Medium (Requires robust optimization)	High (Simulation-based feedback)
Autonomous Ship Support	None	Low (Centralized only)	Low (Global planning)	High (Agent-based Cooperative Autonomy)
Computational Efficiency	Very High	Low (NP-hard scaling)	Medium (Slow convergence)	Balanced (High throughput / Reasonable time)

611 These results confirm that SMOGA does not merely trade off time for capacity; it improves
 612 both simultaneously compared to other intelligent algorithms. It serves as a strictly dominant
 613 solution against NSGA-II, PSO, ACO, SA, and GWO, validating that fusing high-fidelity
 614 simulation with evolutionary search is the optimal strategy for autonomous port scheduling.



615 **Fig. 15.** Balanced result of different algorithms on three problems

616 **5.4 Discussion**

617 From the experimental results and comparisons in the simulation part, it is evident that our
 618 designed port navigation system simulation model is reliable and effective, closely reflecting the
 619 actual operational conditions of the port. The experimental results from the optimization part
 620 demonstrate that our framework, which integrates simulation and optimization, effectively
 621

622 optimizes traffic organisation. A comparative analysis of the three problems is as follows:

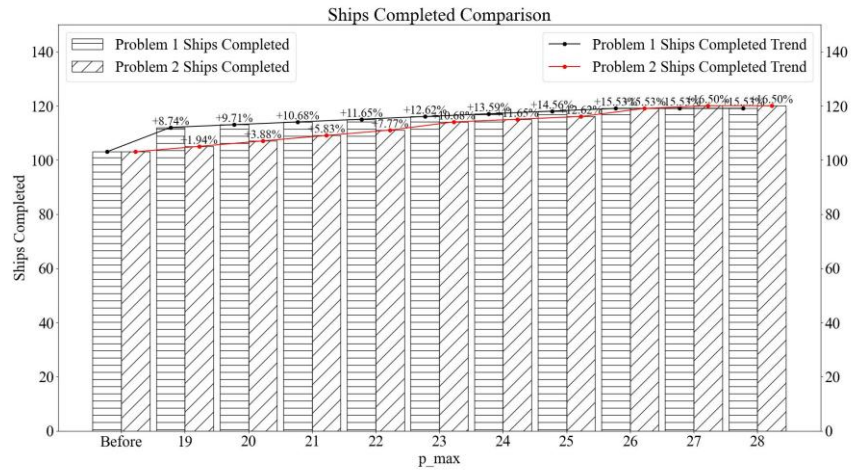
623 Comparing problem 1 and problem 2, it is observed that focusing solely on maximizing the
624 number of ships passing can achieve good optimization results with only a slight increase in p_{max} .
625 However, as p_{max} continues to increase, the optimization effects of the three problems on the
626 maximum number of ships passing are essentially the same in the end (**Fig. 16**). An analysis of the
627 average completion time of ships under the two Problems reveals that in problem 1, which only
628 considers the maximum number of ship completions, the metric of average completion time is
629 overlooked. This leads to an increase in the average completion time of ships in the optimized
630 traffic organisation plan, ranging from 18.65% to 52.72% compared to the pre-optimization plan
631 (**Fig. 17**). However, when average completion time is considered in the optimization problem, this
632 issue is significantly mitigated, and the increase in average completion time is reduced to
633 5.25%-19.05%.

634 By comparing the results of problem 3 with the experimental results of problem 1, it can be
635 observed that there is no significant difference in the number of ships completed at maximum
636 capacity (**Fig. 18**), and the trend of change is essentially the same. However, when comparing the
637 average completion time (**Fig. 17 and 19**), it can be found that after considering economic
638 indicators, the average completion time of ships has actually increased. Therefore, it can be
639 inferred that blindly focusing on the efficiency of port operations may have a negative impact on
640 economy. It is observed that due to the significant optimization potential in the arrival sequence of
641 ships, the optimization focus is primarily on reducing waiting times at anchorages. The
642 optimization algorithm achieves this by reordering the ships' arrival sequence to decrease the time
643 spent waiting at anchorages. In contrast, the waiting time required at berths is subject to resource
644 and process constraints, resulting in limited optimization potential. The experimental results
645 demonstrate that the framework combining simulation with optimization algorithms aligns well
646 with practical scenarios. However, the principle of fairness has been overlooked in the process of
647 rearranging the order of ship arrival (**Fig. 10, Fig. 12 and 14**). It is worth noting that while
648 SMOGA successfully optimizes the comprehensive objective, the average completion time in
649 Problem 3 (considering economic cost) is slightly higher than in Problem 2 (time-only
650 optimization). This is a calculated logical trade-off: to minimize the total Economic Cost (E), the
651 algorithm autonomously prioritizes reducing the usage of expensive auxiliary resources
652 (tugs/pilots) over pure speed. Consequently, some ships are scheduled to wait slightly longer for a
653 “cheaper” time window where resource contention is lower, thereby sacrificing marginal time
654 efficiency to achieve optimal economic viability

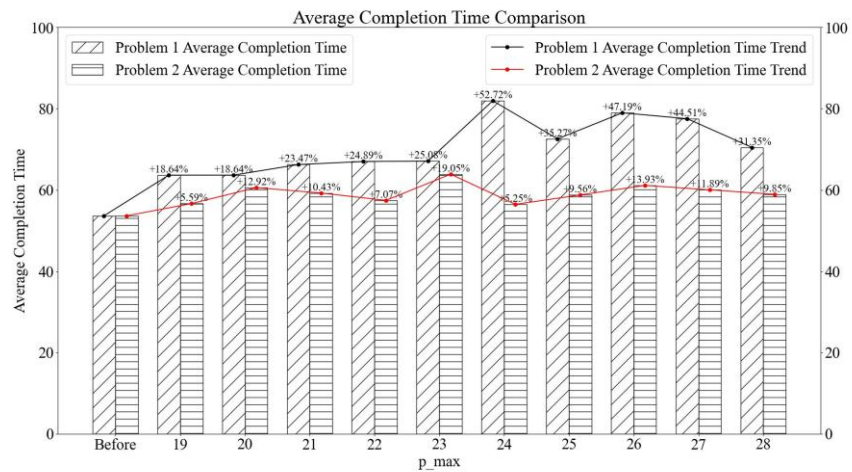
655 The “Autonomous Organization” capability of the proposed system is concretely manifested
656 in the elimination of passive waiting times. As observed in the initial schedules (**Figs. 10a, 12a,**
657 **and 14a**), approximately 30% to 50% of vessels were compelled to wait at the anchorage due to
658 resource contention and uncoordinated arrivals. However, the SMOGA framework autonomously
659 re-sequenced the vessel entry order without human intervention. The impact is evident in the
660 optimized results (**Figs. 10b, 12b, and 14b**), where anchorage waiting times were almost
661 completely eliminated for all ships. The only exception occurred in Scenario 3 (**Fig. 14b**), where a
662 single vessel retained a brief waiting period due to tight economic constraints. This drastic
663 transition—from substantial delays to seamless transit—demonstrates the system's capacity to
664 autonomously resolve conflicts by adjusting temporal sequences.

665 Regarding the system's adaptability to high dynamics, although the current 30-minute
666 computation time precludes instantaneous collision avoidance, it is perfectly suited for Rolling
667 Horizon Optimization (RHO) at the tactical level. In practical deployment, the framework is
668 designed to operate on a sliding window (e.g., updating the schedule every 4 hours for the next
669 12-hour horizon). As new ships arrive or resources change, the Digital Twin absorbs these

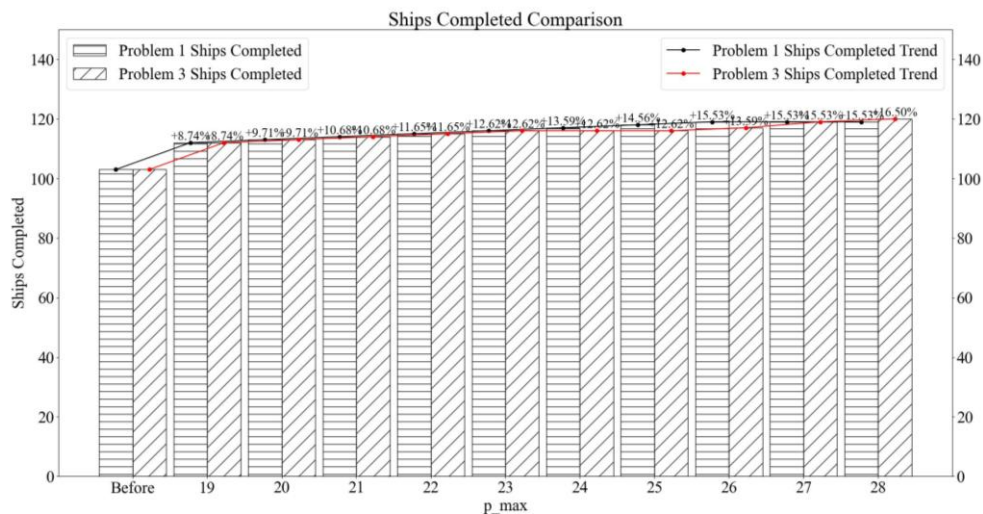
670 deviations, and the SMOGA re-optimizes the subsequent window. This periodic re-planning
 671 ensures that the “Traffic Organization” remains robust against the stochastic nature of maritime
 672 traffic without requiring second-level latency.



673
 674 **Fig. 16.** Comparison of the optimization results of the number of completed ships under problem
 675 1&2



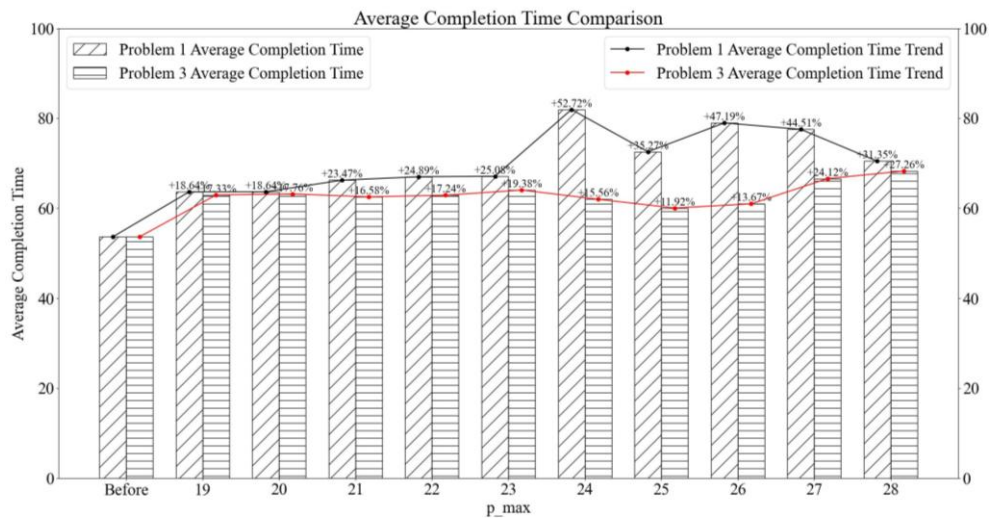
676
 677 **Fig. 17.** Comparison of the optimization results of the average ship navigation time under problem
 678 1&2



679

680
681

Fig. 18. Comparison of the optimization results of the number of completed ships under problem 1&3



682
683
684

Fig. 19. Comparison of the optimization results of the number of completed ships under problem 1&3

685 6. Conclusion and future work

686 The transition towards autonomous port systems presents unique challenges that traditional
687 static scheduling models fail to address, particularly regarding stochastic uncertainties and
688 dynamic resource coupling. This study proposes an Intelligent Traffic Organization framework
689 that bridges the gap between mathematical planning and dynamic execution.

690 By fusing a MIP formulation with a high-fidelity digital twin, the proposed framework
691 effectively solves the “pain point” of rigid scheduling. Unlike traditional MIP models that often
692 collapse under the unpredictability of ocean conditions, our Simulation-based Multi-Objective
693 Genetic Algorithm (SMOGA) utilizes a cooperative autonomy mechanism. This allows for the
694 fusion of heterogeneous data streams—from vessel trajectories to pilot availability—into a unified,
695 robust decision space.

696 The experimental validation at Tianjin Port demonstrates that the proposed method
697 significantly outperforms traditional rules and standard meta-heuristics. By shifting from static
698 rule-based management to evolutionary autonomous optimization, the system increases
699 throughput by 16.5% and reduces vessel turnaround time by 11.7%. This research provides a
700 viable pathway for realizing robust, autonomous decision-making in the next generation of smart
701 ports.

702 Acknowledgement

703 This study was supported by the National Natural Science Foundation of China (No.
704 52471383 & 52471381)

705 References

- 706 Abou Kasm, O., Diabat, A., Bierlaire, M., 2021. Vessel scheduling with pilotage and tugging
707 considerations. *Transportation Research Part E: Logistics and Transportation Review* 148,
708 102231. <https://doi.org/10.1016/j.tre.2021.102231>
- 709 Al-Dhaheri, N., Diabat, A., 2017. A Lagrangian relaxation-based heuristic for the multi-ship
710 quay crane scheduling problem with ship stability constraints. *Ann Oper Res* 248, 1–24.
711 <https://doi.org/10.1007/s10479-016-2239-8>
- 712 Aydogdu, Y.V., Yurtoren, C., Park, J.-S., Park, Y.-S., 2012. A Study on Local Traffic

713 Management to Improve Marine Traffic Safety in the Istanbul Strait. *The Journal of*
714 *Navigation* 65, 99–112. <https://doi.org/10.1017/S0373463311000555>

715 Chen, L., Qi, J., Shi, J., 2023. A cellular automata ship traffic flow model considering navigation
716 rules in narrowing channel. *Alexandria Engineering Journal* 69, 715–726.
717 <https://doi.org/10.1016/j.aej.2023.01.062>

718 Chen, W., Chen, J., Geng, J., Ye, J., Yan, T., Shi, J., Xu, J., 2023. Monitoring and evaluation of
719 ship operation congestion status at container ports based on AIS data. *Ocean & Coastal*
720 *Management* 245, 106836. <https://doi.org/10.1016/j.ocecoaman.2023.106836>

721 Corry, P., Bierwirth, C., 2019. The Berth Allocation Problem with Channel Restrictions.
722 *Transportation Science* 53, 708–727. <https://doi.org/10.1287/trsc.2018.0865>

723 Fagerholt, K., 2001. Ship scheduling with soft time windows: An optimisation based approach.
724 *European Journal of Operational Research* 131, 559–571.
725 [https://doi.org/10.1016/S0377-2217\(00\)00098-9](https://doi.org/10.1016/S0377-2217(00)00098-9)

726 Fan, Q., Jin, Y., Wang, W., Yan, X., 2019. A performance-driven multi-algorithm selection
727 strategy for energy consumption optimization of sea-rail intermodal transportation. *Swarm*
728 *and Evolutionary Computation* 44, 1–17. <https://doi.org/10.1016/j.swevo.2018.11.007>

729 Fan, R., Lu, J., Wang, D.Z.W., Li, M., Liu, Q., 2025. Group-benefit control strategy for
730 connected automated vehicles in mixed traffic at intersections. *Transportation Research Part*
731 *C: Emerging Technologies* 175, 105121. <https://doi.org/10.1016/j.trc.2025.105121>

732 Hsu, H.-P., 2016. A HPSO for solving dynamic and discrete berth allocation problem and
733 dynamic quay crane assignment problem simultaneously. *Swarm and Evolutionary*
734 *Computation* 27, 156–168. <https://doi.org/10.1016/j.swevo.2015.11.002>

735 Hu, H., Chen, X., Sun, Z., 2017. Effect of Water Flows on Ship Traffic in Narrow Water
736 Channels Based on Cellular Automata. *Polish Maritime Research* 24.
737 <https://doi.org/10.1515/pomr-2017-0115>

738 Jia, S., Li, C.-L., Xu, Z., 2020. A simulation optimization method for deep-sea vessel berth
739 planning and feeder arrival scheduling at a container port. *Transportation Research Part B:*
740 *Methodological* 142, 174–196. <https://doi.org/10.1016/j.trb.2020.10.007>

741 Jia, S., Li, C.-L., Xu, Z., 2019. Managing Navigation Channel Traffic and Anchorage Area
742 Utilization of a Container Port. *Transportation Science* 53, 728–745.
743 <https://doi.org/10.1287/trsc.2018.0879>

744 Jia, S., Meng, Q., Kuang, H., 2022. Equitable Vessel Traffic Scheduling in a Seaport.
745 *Transportation Science* 56, 162–181. <https://doi.org/10.1287/trsc.2021.1076>

746 Jiang, L., Huang, G., Huang, C., Wang, W., 2019. Data Mining and Optimization of a Port Vessel
747 Behavior Behavioral Model Under the Internet of Things. *IEEE Access* 7, 139970–139983.
748 <https://doi.org/10.1109/ACCESS.2019.2943654>

749 Jin, J., Huang, H., Li, Y., Zhang, G., Dong, Y., Zhou, B., Xue, H., 2025. Variable speed limit
750 modelling to improve traffic safety and efficiency of mixed traffic flow by a two-stage
751 framework. *Transportmetrica A: Transport Science* 21, 2253476.
752 <https://doi.org/10.1080/23249935.2023.2253476>

753 Kang, L., Meng, Q., Tan, K.C., 2020. Tugboat scheduling under ship arrival and tugging process
754 time uncertainty. *Transportation Research Part E: Logistics and Transportation Review* 144,

755 102125. <https://doi.org/10.1016/j.tre.2020.102125>

756 Karimi, N., Javanmardi, E., Nadaffard, A., Facchini, F., 2025. Systematic analysis and
757 optimization of operational delay factors in port supply chains using a hybrid
758 DEMATEL-OPA-DGRA approach. *Ocean & Coastal Management* 263, 107620.
759 <https://doi.org/10.1016/j.ocecoaman.2025.107620>

760 Kawaguchi, A., Inaishi, M., Kondo, H., Kondo, M., 2009. Towards the development of
761 intelligent navigation support systems for group shipping and global marine traffic control.
762 *IET Intelligent Transport Systems* 3, 257–267. <https://doi.org/10.1049/iet-its.2008.0080>

763 Ksciuk, J., Kuhlemann, S., Tierney, K., Koberstein, A., 2023. Uncertainty in maritime ship
764 routing and scheduling: A Literature review. *European Journal of Operational Research* 308,
765 499–524. <https://doi.org/10.1016/j.ejor.2022.08.006>

766 Li, L., Wang, C., Zhang, Y., Qu, X., Li, R., Chen, Z., Ran, B., 2022. Microscopic state evolution
767 model of mixed traffic flow based on potential field theory. *Physica A: Statistical Mechanics*
768 *and its Applications* 607, 128185. <https://doi.org/10.1016/j.physa.2022.128185>

769 Li, M., Xie, C., Li, X., Karoonsoontawong, A., Ge, Y.-E., 2022. Robust liner ship routing and
770 scheduling schemes under uncertain weather and ocean conditions. *Transportation Research*
771 *Part C: Emerging Technologies* 137, 103593. <https://doi.org/10.1016/j.trc.2022.103593>

772 Li, S., Jia, S., 2019. The seaport traffic scheduling problem: Formulations and a column-row
773 generation algorithm. *Transportation Research Part B: Methodological* 128, 158–184.
774 <https://doi.org/10.1016/j.trb.2019.08.003>

775 Liang, M., Liu, K., Gao, R., Li, Y., 2025. Integrating GPU-Accelerated for Fast Large-Scale
776 Vessel Trajectories Visualization in Maritime IoT Systems. *IEEE Transactions on Intelligent*
777 *Transportation Systems* 26, 4048–4065. <https://doi.org/10.1109/TITS.2024.3521050>

778 Liu, B., Li, Z.-C., Sheng, D., Wang, Y., 2021a. Integrated planning of berth allocation and vessel
779 sequencing in a seaport with one-way navigation channel. *Transportation Research Part B:*
780 *Methodological* 143, 23–47. <https://doi.org/10.1016/j.trb.2020.10.010>

781 Liu, B., Li, Z.-C., Wang, Y., Sheng, D., 2021b. Short-term berth planning and ship scheduling
782 for a busy seaport with channel restrictions. *Transportation Research Part E: Logistics and*
783 *Transportation Review* 154, 102467. <https://doi.org/10.1016/j.tre.2021.102467>

784 Liu, J., Liu, Y., Qi, L., 2021. Modelling liquefied natural gas ship traffic in port based on cellular
785 automaton and multi-agent system. *The Journal of Navigation* 74, 533–548.
786 <https://doi.org/10.1017/S0373463321000059>

787 Liu, J., Zhou, F., Wang, M., 2010. Simulation of Waterway Traffic Flow at Harbor Based on the
788 Ship Behavior and Cellular Automata, in: 2010 International Conference on Artificial
789 Intelligence and Computational Intelligence. Presented at the 2010 International Conference
790 on Artificial Intelligence and Computational Intelligence, pp. 542–546.
791 <https://doi.org/10.1109/AICI.2010.352>

792 Liu, R.W., Guo, Y., Lu, Y., Chui, K.T., Gupta, B.B., 2023. Deep Network-Enabled Haze
793 Visibility Enhancement for Visual IoT-Driven Intelligent Transportation Systems. *IEEE*
794 *Transactions on Industrial Informatics* 19, 1581–1591.
795 <https://doi.org/10.1109/TII.2022.3170594>

796 Liu, R.W., Guo, Y., Nie, J., Hu, Q., Xiong, Z., Yu, H., Guizani, M., 2022a. Intelligent

797 Edge-Enabled Efficient Multi-Source Data Fusion for Autonomous Surface Vehicles in
798 Maritime Internet of Things. *IEEE Transactions on Green Communications and Networking*
799 6, 1574–1587. <https://doi.org/10.1109/TGCN.2022.3158004>

800 Liu, R.W., Liang, M., Nie, J., Lim, W.Y.B., Zhang, Y., Guizani, M., 2022b. Deep
801 Learning-Powered Vessel Trajectory Prediction for Improving Smart Traffic Services in
802 Maritime Internet of Things. *IEEE Transactions on Network Science and Engineering* 9,
803 3080–3094. <https://doi.org/10.1109/TNSE.2022.3140529>

804 Liu, Yang, Liu, J., Liu, Yi, Zhang, Q., Shu, J., Zhang, Y., 2024a. Simulation modelling and
805 analysis of linkage-controlled traffic scheme in waterway transport key nodes. *Simulation*
806 *Modelling Practice and Theory* 102958. <https://doi.org/10.1016/j.simpat.2024.102958>

807 Liu, Yang, Liu, J., Zhang, Q., Liu, Yi, Wang, Y., 2024b. Effect of dynamic safety distance of
808 heterogeneous traffic flows on ship traffic efficiency: A prediction and simulation approach.
809 *Ocean Engineering* 294, 116660. <https://doi.org/10.1016/j.oceaneng.2023.116660>

810 Liu, Yang, Liu, J., Zhang, Q., Liu, Yi, Wang, Y., Yang, L., 2025. Maritime IoT-oriented ship
811 speed prediction: Integrating adaptive wavelet analysis and attention-based uncertainty
812 modelling. *Regional Studies in Marine Science* 91, 104574.
813 <https://doi.org/10.1016/j.rsma.2025.104574>

814 Lu, Y., Guo, Y., Liu, R.W., Ren, W., 2022. MTRBNet: Multi-Branch Topology Residual
815 Block-Based Network for Low-Light Enhancement. *IEEE Signal Processing Letters* 29,
816 1127–1131. <https://doi.org/10.1109/LSP.2022.3162145>

817 Lu, Y., Yang, D., Gao, Y., Liu, R.W., Liu, J., Guo, Y., 2024. AoSRNet: All-in-One Scene
818 Recovery Networks via multi-knowledge integration. *Knowledge-Based Systems* 294,
819 111786. <https://doi.org/10.1016/j.knosys.2024.111786>

820 Luo, X., Yan, R., Wang, S., 2024. Ship sailing speed optimization considering dynamic
821 meteorological conditions. *Transportation Research Part C: Emerging Technologies* 167,
822 104827. <https://doi.org/10.1016/j.trc.2024.104827>

823 Ma, Q., Tang, H., Liu, C., Zhang, M., Zhang, D., Liu, Z., Zhang, L., 2024. A big data analytics
824 method for the evaluation of maritime traffic safety using automatic identification system
825 data. *Ocean & Coastal Management* 251, 107077.
826 <https://doi.org/10.1016/j.ocecoaman.2024.107077>

827 Norstad, I., Fagerholt, K., Laporte, G., 2011. Tramp ship routing and scheduling with speed
828 optimization. *Transportation Research Part C: Emerging Technologies, Freight*
829 *Transportation and Logistics (selected papers from ODYSSEUS 2009 - the 4th International*
830 *Workshop on Freight Transportation and Logistics)* 19, 853–865.
831 <https://doi.org/10.1016/j.trc.2010.05.001>

832 Psaraftis, H.N., Kontovas, C.A., 2014. Ship speed optimization: Concepts, models and combined
833 speed-routing scenarios. *Transportation Research Part C: Emerging Technologies* 44, 52–69.
834 <https://doi.org/10.1016/j.trc.2014.03.001>

835 Qi, L., Ji, Y., Balling, R., Xu, W., 2021. A cellular automaton-based model of ship traffic flow in
836 busy waterways. *The Journal of Navigation* 74, 605–618.
837 <https://doi.org/10.1017/S0373463320000636>

838 Qi, L., Zheng, Z., Gang, L., 2017. A cellular automaton model for ship traffic flow in waterways.

839 Physica A: Statistical Mechanics and its Applications 471, 705–717.
840 <https://doi.org/10.1016/j.physa.2016.12.028>

841 Qu, X., Meng, Q., 2012. The economic importance of the Straits of Malacca and Singapore: An
842 extreme-scenario analysis. *Transportation Research Part E: Logistics and Transportation*
843 *Review*, Select Papers from the 19th International Symposium on Transportation and Traffic
844 *Theory* 48, 258–265. <https://doi.org/10.1016/j.tre.2011.08.005>

845 Shu, Y., Xiong, C., Zhu, Y., Liu, K., Liu, R.W., Xu, F., Gan, L., Zhang, L., 2024. Reference path
846 for ships in ports and waterways based on optimal control. *Ocean & Coastal Management*
847 253, 107168. <https://doi.org/10.1016/j.ocecoaman.2024.107168>

848 Smierzchalski, R., Michalewicz, Z., 2000. Modeling of ship trajectory in collision situations by
849 an evolutionary algorithm. *IEEE Transactions on Evolutionary Computation* 4, 227–241.
850 <https://doi.org/10.1109/4235.873234>

851 Sun, Y., Bai, D., Han, G., Feng, R., Hao, J., Yao, B., 2025. Resilience maintenance strategy for
852 mixed vehicle traffic on port expressway based on lane management. *Ocean & Coastal*
853 *Management* 265, 107645. <https://doi.org/10.1016/j.ocecoaman.2025.107645>

854 Sun, Z., Chen, Z., Hu, H., Zheng, J., 2015. Ship interaction in narrow water channels: A two-lane
855 cellular automata approach. *Physica A: Statistical Mechanics and its Applications* 431, 46–51.
856 <https://doi.org/10.1016/j.physa.2015.02.079>

857 Towards a green and just transition, 2023. , *Review of maritime transport / United Nations*
858 *Conference on Trade and Development*, Geneva. United Nations, Geneva.

859 Wang, C., Zhang, X., Gao, H., Bashir, M., Li, H., Yang, Z., 2024. Optimizing anti-collision
860 strategy for MASS: A safe reinforcement learning approach to improve maritime traffic
861 safety. *Ocean & Coastal Management* 253, 107161.
862 <https://doi.org/10.1016/j.ocecoaman.2024.107161>

863 Wang, Y., Liu, R.W., Liu, J., Yang, L., Liu, Y., Piera Eroles, M.A., 2026. Resilient RoRo fleet
864 scheduling for mixed EV and ICEV transport demand: An optimization framework for EV
865 dedicated service strategy. *Transportation Research Part E: Logistics and Transportation*
866 *Review* 209, 104719. <https://doi.org/10.1016/j.tre.2026.104719>

867 Wang, Y., Meng, Q., Kuang, H., 2018. Jointly optimizing ship sailing speed and bunker purchase
868 in liner shipping with distribution-free stochastic bunker prices. *Transportation Research Part*
869 *C: Emerging Technologies* 89, 35–52. <https://doi.org/10.1016/j.trc.2018.01.020>

870 Wei, X., Jia, S., Meng, Q., Tan, K.C., 2020. Tugboat scheduling for container ports.
871 *Transportation Research Part E: Logistics and Transportation Review* 142, 102071.
872 <https://doi.org/10.1016/j.tre.2020.102071>

873 Wu, L., Jia, S., Wang, S., 2020. Pilotage planning in seaports. *European Journal of Operational*
874 *Research* 287, 90–105. <https://doi.org/10.1016/j.ejor.2020.05.009>

875 Xia, Z., Guo, Z., Wang, W., Jiang, Y., 2021. Joint optimization of ship scheduling and speed
876 reduction: A new strategy considering high transport efficiency and low carbon of ships in
877 port. *Ocean Engineering* 233, 109224. <https://doi.org/10.1016/j.oceaneng.2021.109224>

878 Xiao, Y., Li, X., Yin, J., Liang, W., Hu, Y., 2023. Adaptive multi-source data fusion vessel
879 trajectory prediction model for intelligent maritime traffic. *Knowledge-Based Systems* 277,
880 110799. <https://doi.org/10.1016/j.knosys.2023.110799>

881 Yan, R., Liu, Y., Wang, S., 2024. A data-driven optimization approach to improving maritime
882 transport efficiency. *Transportation Research Part B: Methodological* 180, 102887.
883 <https://doi.org/10.1016/j.trb.2024.102887>

884 Yang, Y., Yan, R., Wang, S., 2024. An efficient ranking-based data-driven model for ship
885 inspection optimization. *Transportation Research Part C: Emerging Technologies* 165,
886 104731. <https://doi.org/10.1016/j.trc.2024.104731>

887 Yao, Z., Wu, Y., Wang, Y., Zhao, B., Jiang, Y., 2023. Analysis of the impact of maximum platoon
888 size of CAVs on mixed traffic flow: An analytical and simulation method. *Transportation*
889 *Research Part C: Emerging Technologies* 147, 103989.
890 <https://doi.org/10.1016/j.trc.2022.103989>

891 Zhang, F., Li, J., Zhao, Q., 2005. Single-lane traffic simulation with multi-agent system, in:
892 *Proceedings. 2005 IEEE Intelligent Transportation Systems, 2005. Presented at the*
893 *Proceedings. 2005 IEEE Intelligent Transportation Systems, 2005.*, pp. 56–60.
894 <https://doi.org/10.1109/ITSC.2005.1520219>

895 Zhen, L., Hu, Z., Yan, R., Zhuge, D., Wang, S., 2020. Route and speed optimization for liner
896 ships under emission control policies. *Transportation Research Part C: Emerging*
897 *Technologies* 110, 330–345. <https://doi.org/10.1016/j.trc.2019.11.004>

898 Zhen, R., Jin, Y., Hu, Q., Shao, Z., Nikitakos, N., 2017. Maritime Anomaly Detection within
899 Coastal Waters Based on Vessel Trajectory Clustering and Naïve Bayes Classifier. *J.*
900 *Navigation* 70, 648–670. <https://doi.org/10.1017/S0373463316000850>

901